BIOLUMINESCENT IMAGING OF AN NF-kB TRANSGENIC MOUSE MODEL FOR MONITORING IMMUNE RESPONSE TO A BIOARTIFICIAL PANCREAS REAL TIME AND *IN VIVO*: VALIDATION OF THE METHOD

By

David Roth

Thesis

Submitted to the Faculty of the

Graduate School of Vanderbilt University

in partial fulfillment of the requirements

for the degree of

MASTER OF SCIENCE

in

Biomedical Engineering

May, 2005

Nashville, Tennessee

Approved:

Professor Taylor G. Wang

Professor Frederick R. Haselton

ACKNOWLEDGEMENTS

I would like to thank my advisor, Taylor Wang, for his guidance in this research. I would also like to thank those whose expertise helped the completion of this project, Al Powers, Duco Jansen, Rick Haselton, Michael Fowler, Timothy Blackwell, and Fiona Yull.

I would also like to credit both the Juvenile Diabetes Foundation and the National Aeronautics and Space Administration.

Thank you to my family and friends for your support.

TABLE OF CONTENTS

Page

LIST OF TABLES

Table Page

LIST OF FIGURES

CHAPTER I

INTRODUCTION

There are a number of therapies used for the treatment of Type I Diabetes Mellitus, but no cure. They can include daily insulin injections, organ transplantation, islet transplantation, and cellular encapsulation. Cellular encapsulation is a novel approach for the treatment of several pathologies, including diabetes. Capsules are fabricated using alginate, a crude product polysaccharide comprised of mannuronic and guluronic acid residues acquired from alga [1]. Many variables need to be controlled during the fabrication of these alginate-based capsules such as mechanical strength, pore size, and biocompatibility. Until now, biocompatibility measurements of the bioartifical pancreas have been made histologically, which allows for considerable biological variability and difficulty in constructing a timeline of immune response because only one data point can be obtained per animal. For this experiment, *in vivo* bioluminescence imaging using a Nuclear Factor-kappa Beta (NF-kB) marker allows unlimited measurements of biocompatibility to be made in real time. NF-kB is a transcription factor that plays a critical upstream role in coordinating the inflammatory and wound healing cascade. Acquiring information from the same mouse repeatedly to construct a time line of immune response allows each new data point an accurate reference to the last, instead of relying on data points acquired from different animals. This is in part made possible because each mouse can be used as its own control. The requirement for fewer animals

reduces the reliance on statistical analysis and increases the importance of real time data. Collected data can reveal important information about the immune response time course.

The ultimate goal of diabetic reversal is to mimic metabolic control of blood/glucose levels. In a non-diabetic patient, insulin-producing beta cells are able to monitor and respond to glucose fluctuations continuously. Daily insulin injection is the most common therapy for type I diabetes mellitus, but complications from the lack of continuous blood/glucose regulation can occur. Most diabetic patients inject nearly four times daily. Bolus insulin injections do not accurately reflect endogenous insulin release in non-diabetic patients. Deviations from this control can result in hyperglycemia, whose complications over time can involve vessel wall deterioration and is a source of more serious diabetic ailments such as cardiovascular and renal disease. Even the most responsible diabetic patient is susceptible to the limitations of insulin injection therapy.

Ideally, organ and islet transplantations should be able to imitate metabolic control of blood/glucose regulation, and success has been made [2]. However, secondary immunosuppressive side effects such as mucosal ulcers, malaise, risks of infection, and tumors, still hamper long-term efficacy of the transplantation. Steroids can induce graft failure, and other immunosuppressive drugs can be toxic to the islet cells and induce peripheral insulin resistance [2-4]. Some relevant areas of research attempting to circumvent the foreign tissue rejection problem are donor bone marrow infusion for tolerance induction, and use of monoclonal anti-bodies to impede co-stimulatory pathways of immune rejection [3, 5].

Lack of donor sources is a major impedance to the success of organ and islet transplantation. Research has shown that an average of two pancreata worth of islets is

necessary for diabetic reversal, doubling the number of human resources necessary to treat just one [2-4]. Conversely, there are many islet sources for xenograft transplantations. Xenograft tolerance is more difficult to attain than the allograft tolerance whose success is still not completely resolved. Cellular encapsulation offers an approach to the transplantation of allo- or xeno-islet cells without rejection or autoimmune complications [6]. Islet cells are sequestered inside alginate-based capsules whose walls have pores, approximately 72 kilodaltons, large enough for nutrients and hormone to diffuse, but small enough so the host immune system cannot reject the foreign cells inside. Cellular encapsulation offers a means of circumventing immunosuppression and allowing islets to continuously monitor and adjust blood/glucose levels. There is inherent lag in the regulation of blood/glucose levels, as signals from the blood must diffuse through the capsule semi-permeable membrane to interact with the islets, and resulting hormones must diffuse back into the surrounding system. The extent of this temporal distortion differs depending on the methods and materials used to construct the capsules, and attempts to make responses instantaneous are being made. Lim and Sun, the first to pioneer microencapsulation for the use as a bioartificial pancreas, show an insulin release time delay of approximately 7 minutes after glucose load in vitro [7]. Cellular encapsulation is a promising solution to both the immunosuppression and limited allograft donor source dilemma.

Many variables such as size, mechanical strength, and diffusivity need to be accurately controlled during the fabrication of these alginate-based capsules. In addition, especially for transplantation purposes, it is important to regulate biocompatibility. Particularly non-biocompatible capsules can elicit fibrosis on the capsule wall capable of

causing islet necrosis [8-10]. Even empty capsules, without sequestered islet cells inside, have been shown to elicit immune responses. Several experiments have been conducted to quantify this, all using similar techniques. Capsules are fabricated and then implanted into the peritoneal cavity of mice. They are allowed to incubate for specified periods of time and are then recovered via peritoneal lavage. Capsules are examined for integrity and for the number of immune response cells in the area or adhered to the capsule walls. Labs then create quantitative scales to score the biocompatibility of the capsules based on their observations [1, 8-14]. Appropriate for these procedures, biocompatibility can be defined as the number of cells or cell layers surrounding the retrieved capsules. There are several disadvantages to these methods. A time line of immune response is hard to determine unless many animals are used because only one data point can be obtained per animal. Using many mice introduces sources of variance in data owing to inherent biological variability between the animals.

To circumvent these problems, we propose an alternate method of monitoring immune response. *In vivo* bioluminescence imaging allows measurements of immune response to be acquired in real time. Transgenic mice expressing luciferase under the control of the proximal 5' human immunodeficiency virus long terminal repeat, a known NF-kB dependent promoter sequence, are used. NF-kB initiates the transcription of many cytokines, chemokines, adhesion molecules, and proinflammatory genes [15-18]. When NF-kB binds to its promoter sequence to initiate transcription of immune response proteins, luciferase is also produced. Luciferase, in conjunction with its substrate, luciferin, catalyzes a bioluminescent reaction detectable by a sensitive charge coupled device camera. The amount of light (photons/sec/cm^2/sr) detected by the camera is

therefore indicative of NF-kB activity, which is highly involved in regulating the immune response in not only the murine animal model, but humans as well [16, 18-21].

Immune Response

Immune response to implant materials can be initiated a number of ways. One of the simplest interactions occurs when ions, fluids, or pieces of the implant material is absorbed by the surrounding tissue, a phenomenon known as leaching. Likewise, swelling can occur when implant materials absorb ions or fluids from surrounding tissue. Both of these phenomenons are a result of diffusion, and occur after capsule transplantation [22]. Specific to the procedures conducted in this experiment, the event that first triggers immune response is trauma due to surgery. Natural killer cells of the host immune system act not only to cleanse the body of implanted foreign molecules, but local dead cells and cell fragments as well, of which there are many around the site of surgery and implantation.

There exist a number of specific and non-specific mechanisms the human body uses to defend against foreign pathogens. Non-specific mechanisms require various phagocytic white cells and natural killer cells. There are two specific immune responses the body can engage to defend against all pathogens; one is a humoral response and the other a cell-mediated response. The reactions differ primarily on the location of pathogens; a humoral response is in response to pathogens in body fluids and a cell-mediated response is mounted against intracellular pathogens. Transplantation of a bio-artificial pancreas elicits both non-specific defenses against the implant materials, and primarily a specific humoral immune response if the sequestered islet cells are exposed to

the biological environment. This exposure can happen one of two ways. Capsule wall deterioration can expose the islet cells, and flawed encapsulation techniques can allow islet cells to become trapped in the capsule wall instead of being completely sequestered inside.

The inflammatory cascade begins with rapid dilation of capillaries, which leads to an increase in blood flow volume. There is also an increase in vascular wall permeability, which allows more fluid and cells to permeate into the surrounding tissue. These are precursory events that lead to mounting of the cellular invasion phase of the immune response.

To foster the increase in endothelial cell permeability, endothelial cells become "sticky" by the increase in adhesion molecule expression, which is initiated by NF-kB dependent cytokines IL-1 and TNF-α. The first step, rolling, is the initiation of the expression of endothelial selectins, proteins expressed on endothelial cell surfaces that promote weak interactions with leukocytes in the blood. The expression of these proteins is in part regulated by the NF-kB transcription factor [23-25]. The result is a slowing of immune response cells in the blood around the site of inflammation. The second step is the expression of β2, and eventually β1-integrins on leukocyte surfaces that ultimately foster the migration of leukocytes across the basement membrane. The expression of integrin proteins on leukocytes is partly under NF-kB control, but the translocation of the monocytes across the endothelial wall is also dependant on specific NF-kB dependant cytokines and chemokines [26, 27].

Chemotaxins, or chemoattractants, are polypeptide ligands responsible for amassing leukocytes. Chemoattractant concentration gradients trigger the extravasation

of those cells from the blood. Chemokines attract neutrophils to inflammatory sites via gradient-dependent enhancement of integrin dependent adhesion. For example, NF-kB dependent chemokine IL-8 is secreted by activated endothelial cells and bound to surface glycoproteins in a gradient dependent manner. Neutrophils already involved in selectin rolling are stimulated by IL-8 to express β2-integrins. These integrins in turn bind to ICAM1 endothelial counter-receptors, which are expressed in a gradient dependant manner as well. ICAM1 receptor expression is triggered by proinflammatory NF-kB dependant cytokines such as IL-1 and TNF-α [27]. Immune response cells migrate along the ICAM1 gradient from the endothelium into inflamed tissue via a process known as haptotaxis. There also exist monocyte chemotaxins that are selectively chemotactic for mononuclear leukocytes such as monocytes, macrophages, and lymphocytes.

These steps are necessary to mount the cellular invasion phase of the immune process. There are a number of phagocytic leukocytes and natural killer cells that defend the body non-specifically. Non-specificity implies that cells do not discriminate on the particular pathogen; they will digest any number of different pathogens regardless of their cell-surface markers. No antibodies specific for the particular antigen are produced. Leukocytes depend primarily on phagocytosis to eliminate the pathogen. This process requires engulfing and digestion of fragments using digestive enzymes called lyzozymes, which are stored in cytoplasmic granules. Neutrophils, the first cells to appear at the site of injury, compromise approximately 65% of white blood cells, under normal physiological conditions, and are attracted to sites of inflammation by chemotaxis [28]. Neutrophils and eosinophils, another phagocytic cell line associated with the first line of defense with neutrophils, both have short life spans, hours in blood and several days in

tissue. Extensive presence of these two cells in an area of trauma can be evidence of chronic inflammation [22]. Monocytes, compromising only 5% of white blood cells, circulate in the blood, and then migrate into tissues to enlarge and change into macrophages, cells intimately involved in the specific humoral immune response.

The next cells to arrive at a site of injury are called monocytes when in the blood. Once in the tissue, they enlarge and become macrophages. There exist specific resident populations of monocytes in tissues such as liver and lung that are able to react more quickly to trauma [16, 29]. Their role is similar to neutrophils, relying on phagocytosis, but because of their increased size, they can digest larger particles. Macrophages are capable of many other functions in addition to digesting pathogens. For example, they can fuse to become large multi-nucleated cells called foreign body giant cells that can digest even larger pathogens than those ingested by single macrophages. Macrophages play not only an important role in non-specific defense against pathogens, but are responsible for critical steps of the specific humoral response as well.

A humoral immune response is dependent on B cells, helper T cells, and macrophages. The process is initiated by the phagocytic response of a macrophage to a foreign pathogen. The macrophage engulfs the pathogen, which is then partially digested. These partially digested fragments are presented on the surface of the macrophage by class II Major Histocompatibility Complex proteins. MHC proteins are self-marker proteins used to identify self and non-self cells. Breakdowns in the processing of MHC proteins and the immune cells that interact with them can result in autoimmune deficiencies. Class I MHC molecules are found on most nucleated cells in the body. Class II MHC molecules are restricted for a few cell types intimately involved with the immune

system, such as macrophages and B cells [28]. Once the pathogen fragments on the Class II MHC proteins are presented on the macrophage cell surface, the cell becomes an antigen-presenting cell (APC).

Unlike macrophages and other non-specific leukocytes, T helper cells bind specifically to certain pathogens'-receptor complexes. A T helper cell, whose receptors are specific for the antigenic determinant presented by Class II MHC proteins on the surface of the APC, will bind to that macrophage. Molecules on the T helper cell called CD4 aid this binding phenomenon [30-32]. CD4 molecules have an affinity for certain molecules on the Class II MHC. Binding of these two cells will activate the T helper cell to replicate, resulting T helper cells still specific for the pathogen ingested by the macrophage.

In order to mount the humoral response, B cells must participate simultaneously with T helper cells and macrophages. As opposed to neutrophils and macrophages that rely on phagocytosis of any pathogen, B cells are stimulated by antigens specific to their cell surface receptors. Each antigen activates a very small fraction of B cells in the body. Once the B cell ingests the antigen, it is partially digested and portions of it are coupled to Class II MHC proteins and the complex migrates and expresses itself on the B cell surface. Cloned T helper cells specific to the antigen ingested by both the macrophage and B cell, binds to the MHC complex on the B cell surface. This binding activates the B cell to replicate into effector cells called plasma cells. These plasma cells create proteins called antibodies, all specific to the antigen. Memory cells are also produced that can mount a second immune response much more quickly the next time the host is exposed to the same antigen.

One mediator that regulates the activation of T helper cells by APCs, and B cells by T helper cells, is the secretion of various cytokines, such as NF-kB dependent IL-1. The NF-kB transcription factor is a crucial upstream regulator of a number of cytokines and chemokines intimately involved in the inflammatory process [16, 18, 20, 29, 33, 34].

NF-kB Transcription Factor

Nuclear Factor kappa-Beta is a transcription factor that regulates gene transcription of various pro-inflammatory cytokines and chemokines [16, 18-20, 29, 33, 34]. In addition, it also enhances the transcription of other genes such as growth factors, immunoreceptors, and adhesion molecules. Abnormal continuous activation of NF-kB has been shown to facilitate tumor growth [33, 34], and is also intimately involved in cell proliferation and differentiation in certain tissue types, demonstrating its ubiquitous nature [21, 35-41]. Various inhibitory proteins and positive/negative feedback loops tightly control NF-kB activity. These methods of regulation are important because cytokines are generally not stored intracellularly, and require production starting with transcription in the nucleus. As a result, transcription factors play a major role in regulating the inflammatory cascade via cytokine gene regulation. Although NF-kB plays an important role in regulating inflammatory pathways, it is unknown whether it contributes to the differential production of NF-kB dependent cytokines or in the coordination of the production of the resulting proteins [16].

The group of Rel transcription factors is responsible for the regulation of expression of many genes. They are especially involved in regulating those involved in inflammatory and immune responses [21]. The Rel proteins act in protein-protein

interactions, DNA binding, and nuclear localization [17]. Of the many Rel proteins, some include NF-kB1 (p50/p105), NF-kB2 (p52/p100), RelA (p65), c-Rel, and RelB, which in combination with p50 and RelA, can be found in numerous cell types forming several hetero/homodimers. RelA and p50 constitute most of the cellular subunits, and the RelA/p50 heterodimer is the most ubiquitous and powerful activator of NF-kB dependent genes. Rel proteins contain a conserved 300 amino-acid sequence. These dimers bind to DNA at its promoter, a ten or 11 base pair sequence, but only RelA contains a transactivation domain at the C-terminal end that activates transcription. The different variations of NF-kB can function identically to the classic RelA/p50 dimer, and therefore all forms that bind to the NF-kB binding sites are referred to as NF-kB [16].

The inactive form of NF-kB is sequestered in the cytoplasm of the cell (most information about NF-kB is derived from immune response cells such as lymphocytes, monocytes, and macrophages). Activation occurs when inhibitory proteins are phosphorylated, allowing NF-kB localization signals to relocate the dimer to the nucleus. Phosphorylation can be stimulated by a number of factors including radiation, UV light, chemical agents, viral proteins, bacterial endotoxins, and several cytokines [16]. Not only does the Rel family include select proteins allowing for several hetero/homodimers of NF-kB, but there also exists several inhibitory proteins, known as the IkB family of proteins. They include IkB-α, IkB-ε, IkB-β, and Bcl-3. This inhibitory family contains what is known as an “ankyrin repeat”, a 33 amino acid motif, which gets its name from being abundant in the protein ankyrin [21]. NF-kB inactivity is maintained by binding to I-kB, and although various signals and cell signaling pathways can stimulate NF-kB, most activation results from serine phosphorylation of the I-kB kinase complex. All of

these various dimers and inhibitory proteins highlight the complexities involved in regulating NF-kB dependent gene regulation.

Positive and negative feedback loops help to regulate NF-kB activation both intracellularly and extracellularly. Positive extracellular feedback control can occur, for example, when TNF-α and IL-1β are produced. The production of these cytokines requires NF-kB activation, and in turn, these cytokines activate NF-kB, amplifying the signal. Both intracellular and extracellular negative feedback control can occur, too. The IkB-α and p105 genes, NF-kB inhibitory units, both have NF-kB responsive elements in their promoter sequences. Increased p105 production also means increased p50 homodimer is formed, because p105 is the precursor of the p50 subunit of NF-kB (figure 1).

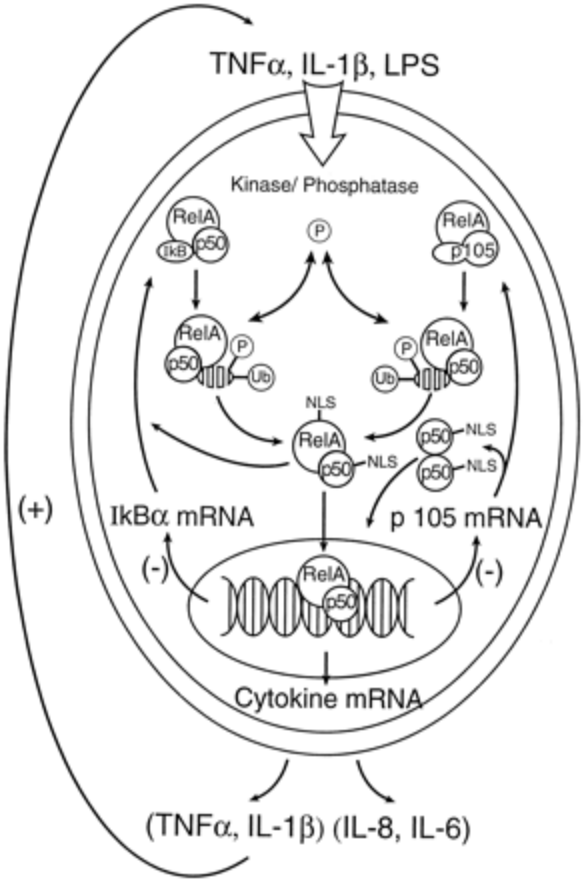

Figure 1. Regulation of NF-kB RelA/p50 dimer after cell stimulation [16].

Since the p50 subunit does not bind the inhibitory protein IkB efficiently, nor does it contain transcription-activating domains, it can efficiently translocate to the nucleus and compete against other NF-kB dimers for NF-kB binding sites. Negative extracellular feedback loops also help to diminish NF-kB activation. Increased TNF- α and IL-1β can produce a counter regulatory cytokine, IL-10. It has been shown that IL-10 can inhibit endotoxin-induced NF-kB activation in monocytes [16]. Synthesis of some, but not all, of both the Rel family of proteins as well as its inhibitors are autoregulated, demonstrating the complexity of NF-kB regulation.

A specific example of this complex inhibitory process has been demonstrated in primary mouse embryo fibroblasts (PMEF). To examine the role of IkB-α, wild-type

(+/+) for IkB-α, heterozygous (+/-), and homozygous null (-/-) fibroblasts were constructed. The null cells did not exhibit constitutive NF-kB activation, as expected, nor was there any increase in NF-kB dependent proteins such as c-Rel, p65, p50, and p105. Therefore, IkB-α does not play a singularly important role in sequestering NF-kB in the cytoplasm of PMEF cells, and other proteins in the inhibitory family are probably responsible. In addition, activation of NF-kB with TNF-α showed increased p65 levels in the wild-type and heterozygous cells, as expected, however, it is unclear which cytoplasmic inhibitor released the transcription factor as p105 and p100 (which can inhibit NF-kB migration) levels did not change, and IkB-β is known not to be responsive to TNF-α [21]. This demonstrates briefly the complexities of NF-kB attenuation and activation in the cytoplasm.

Studies have concluded that protein synthesis is required for termination of an NF-kB response. To determine IkB-α's role in this synthesis, wild type and null PMEFs were used. Each was treated with TNF-α for approximately 30 minutes and then allowed to incubate for 30-60 minutes after withdraw. The wild-type cells returned to basal levels of nuclear p65 about 30 minutes after TNF-α withdraw. However, nuclear p65 levels remained elevated in the null cells, indicating that IkB-α plays a crucial role not in sequestering NF-kB in the cytoplasm, but rather in regulating nuclear levels of p65 after withdraw of an NF-kB activating stimulus [21].

As previously mentioned, it is unknown how responsible the NF-kB motif is for initiating transcription of specific cytokines and chemokines or in helping in the overall coordination of their production. Different cytokines are produced depending on the original signal as well as the tissue type. NF-kB also interacts with several other

transactivators and repressors, as well as promoter-bound transcription factors. As is typical of other transcription factors, NF-kB can have interactions with glucocorticoids that usually inhibit a factor's ability to bind to promoter sequences in the DNA. Different hetero/homodimers can bind to similar binding sites, but with different affinities [42]. These characteristics highlight the complex regulation of cytokine transcription by the NF-kB transcription factor.

Luciferin-Luciferase Complex

Many organisms, such as fireflies, fish, fungi, and bacteria, are capable of emitting light. Each organism emits light for different reasons ranging from communication to mating rituals. The differences in color, ranging from violet (400nm) to red (620 nm), seem to be loosely associated with the habitat in which the organism resides. It has been shown that the enzyme is responsible for the differences in emitted wavelengths [43]. Techniques have been developed to harness this bioluminescence and use it as a biological marker.

All categorized insect luciferases consist of one polypeptide chain ranging from 542-552 amino acid residues. The number of charged amino acid residues is nearly identical, and the main difference is the number of cysteine and tryptophan residues. Various experiments have been performed to determine why shifts in wavelengths exist between nearly homogenous luciferase polypeptide chains across families of insects. For example, for fireflies of the family Luciola, there is an 80% homology for the entire sequence, and a 90% homology for the 250 amino acid residue cluster closest the C-terminus end. However, maximum bioluminescence between the species ranges from

538nm to 622nm. Proposed explanations vary from two stereo conformations of the oxyluciferin complex, to the polarity of specific amino acid residues, to the general effects of the protein microenvironment. At a pH of approximately 7.0, oxyluciferin from fireflies will emit a yellow-green light ranging from 500-700nm, with a peak wavelength at 563nm [44, 45]. These values are both pH and temperature dependent.

Firefly luciferase is an enzyme responsible for the bioluminescence reaction. It catalyzes the oxidation of luciferin in the presence of O_2, ATP, and Mg^{2+}. The first reaction catalyzed by the luciferase is the transformation of luciferin to luciferyl adenylate, with a subsequent release of inorganic pyrophosphate. The luciferase-luciferyl adenylate complex then reacts quickly with the molecular oxygen to produce the keto-form of oxyluciferin, CO_2, and AMP. [15, 44-46] (figure 2).

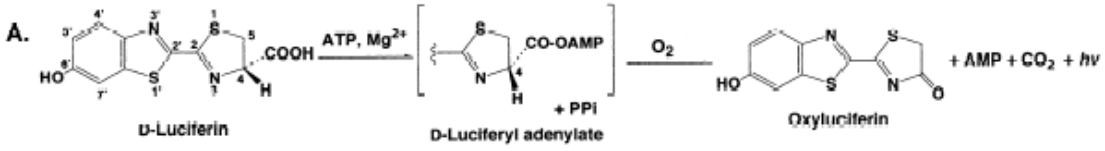

Figure 2. Schematic of bioluminescent reaction [46].

This keto-form of oxyluciferin is an oxyluciferin molecule in a singlet electronically excited state. Proton removal is quick to ensue, transforming the keto-form into the enol form, emitting one quantum of light in the process [44]. One property that makes this bioluminescent reaction unique, and effective for this experiment, is that it does not require excitation energy in the form of light, but rather is chemically driven.

The resulting light is capable of penetrating several centimeters of tissue [15]. A charge-coupled device camera can detect the photons externally. The camera chip and

accompanying software are designed to count the emitted photons per time per area per conic angle. The photon flux, or bioluminescence, is dependent on the amount of luciferase complementary DNA that is transcribed, which is dependent on NF-kB activation. This sequence of events allows this imaging system to be a method of quantifying NF-kB activation, and consequently, immune response.

NF-kB Transgenic Mouse

The transgenic mice used in this experiment are crossed with C57L/J mice. They are housed and bred at Vanderbilt University, Nashville, TN. The mice are engineered to possess the proximal 5' human immunodeficiency virus long terminal repeat, which is a well-documented NF-kB responsive promoter. This promoter sequence, containing a TATA box, drives the expression of *photinus* luciferase complementary DNA [15, 45, 47]. It has been shown in primary cell culture that the NF-kB transcription factor is necessary for the proximal HIV-LTR transcriptional activity [15]. Injection of the substrate luciferin is required for bioluminescence, and is injected intraperitonealy. An example of bioluminescent mice after luciferin injection is shown below (figure 3).

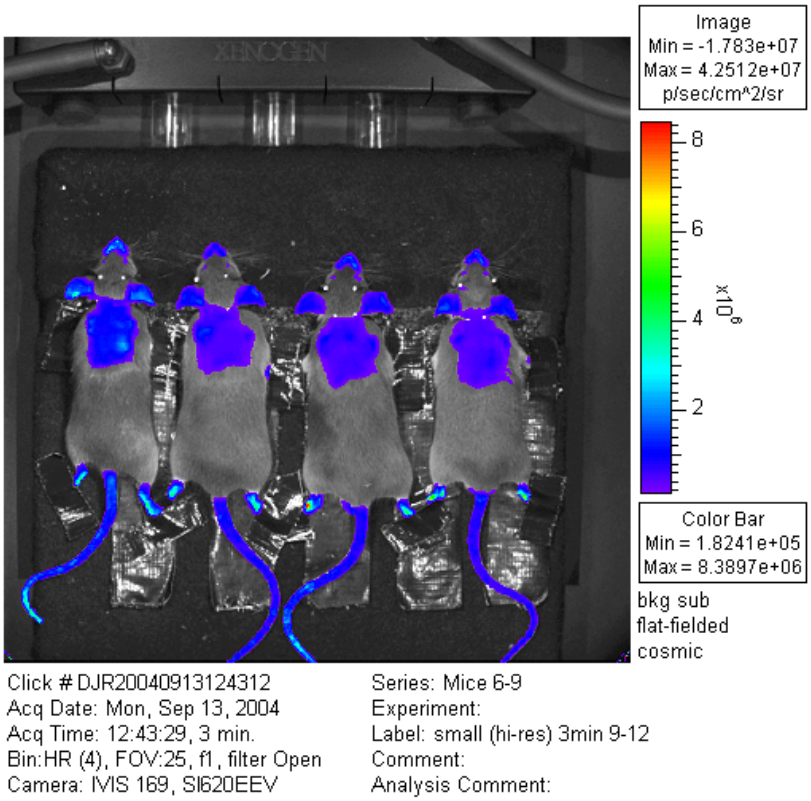

Figure 3. Bioluminescent photograph NF-kB transgenic mice after luciferin injection, dorsal view. Photograph is an overlay of two images, a black and white photograph overlaid with bioluminescent image. Photon counts are acquired from the bioluminescence present at the base of the skull behind the ears, where the dorsal-cervical fat-pad is located. Blue colored region represents bioluminescence. Bioluminescence at dorsal-cervical fat pad is due to post-surgical inflammation to the implants. Bioluminescence of the nose, ears, paws, and tail is due to tissue specific basal NF-kB activity.

These transgenic mice have been used to monitor the effects of dexamethasone treatments on NF-kB activity and lung inflammation [15]. They have also been used to investigate multi-organ inflammatory responses to hepatic cryoablation [45].

CHAPTER II

BIOLUMINESCENT IMAGING OF AN NF-kB TRANSGENIC MOUSE MODEL FOR MONITORING IMMUNE RESPONSE TO A BIOARTIFICIAL PANCREAS REAL TIME AND *IN VIVO:* VALIDATION OF THE METHOD

Abstract

Cell encapsulation is a novel therapeutic approach for the treatment of Type I Diabetes Mellitus that circumvents both the immunosuppression and limited allograft donor source dilemma. Current methods for scoring the biocompatibility of the alginate-based capsules that sequester Islets of Langerhans include fabrication and implantation into the peritoneal cavity of mice, incubation for specified periods of time, retrieval via peritoneal lavage, and observation of the number of cells or cell layers surrounding the capsules. This method allows only one data point to be obtained per animal. In this experiment we propose to measure biocompatibility real time and *in vivo* This new method of monitoring immune response using bioluminescent technology and a Nuclear Factor-kappa Beta sensitive transgenic mouse model allows unlimited data points to be acquired per animal, reduces the number of animals required to obtain statistically significant immune response data over time, and in turn reduces error associated with animal variability. NF-kB is a transcription factor that plays a critical upstream role in the coordination of the inflammatory and would healing cascades by initiating the transcription of many cytokines, chemokines, adhesion molecules, and proinflammatory

genes. Five types of capsules were monitored over 6 six weeks after transplantation into the dorsal-cervical fat pad, a capsule group, a bead group, a non-coated capsule group, a sham surgery group, and a control group. The bead, capsule, and non-coated capsule transplant groups allow the effects of capsule size and capsule wall composition on NF-kB activity to be monitored. This imaging modality was able to detect statistically significant differences in NF-kB activity between pre and post-operative data points per mouse. It was also able to discern with significance an unexpected increase in NF-kB activity due to capsule size instead of capsule wall composition over a six week time period.

Introduction

The ultimate goal of diabetic reversal is to mimic metabolic control of blood/glucose levels. In a non-diabetic patient, insulin-producing beta cells are able to monitor and respond to glucose fluctuations continuously. There are a number of therapies used for the treatment of Type I Diabetes Mellitus, but no cure. They can include daily insulin injections, organ transplantation, islet transplantation, and cellular encapsulation. Cellular encapsulation is a novel approach for the treatment of several pathologies, including diabetes.

Daily insulin injection is the most common therapy for type I diabetes mellitus, but allows complications from the lack of continuous blood/glucose regulation to arise. Ideally, organ and islet transplantations should be able to imitate metabolic control of blood/glucose regulation, and success has been made [2]. However, secondary immunosuppressive side effects such as mucosal ulcers, malaise, risks of infection, and

tumors, still hamper long-term efficacy of the transplantation. Steroids can induce graft failure, and other immunosuppressive drugs can be toxic to the islet cells and induce peripheral insulin resistance [2-4].

Lack of donor sources is a major impediment to the success of organ and islet transplantation. Research has shown that an average of two pancreata worth of islets is necessary for diabetic reversal, doubling the number of human resources necessary to treat just one [2-4]. Cellular encapsulation offers an approach to the transplantation of allo- or xeno-islet cells without rejection or autoimmune complications [6]. Islet cells are sequestered inside alginate-based capsules whose walls have pores large enough for nutrients and hormone to diffuse, but small enough so the host immune system cannot reject the foreign cells inside.

Capsules are fabricated using alginate, a crude product polysaccharide comprised of mannuronic and guluronic acid residues acquired from alga [1]. Many variables need to be controlled during the fabrication of these alginate-based capsules such as mechanical strength, pore size, and biocompatibility. Particularly non-biocompatible capsules can elicit fibrosis on the capsule wall capable of causing islet necrosis [8-10]. Even empty capsules have been shown to elicit immune responses. Until now, procedures for acquiring biocompatibility measurements of the bioartifical pancreas include fabrication and implantation of capsules into the peritoneal cavity of mice, incubation for specified periods of time, and retrieval via peritoneal lavage. Labs create quantitative scales dependant on the number of cells or cell layers adhered to the capsule walls to score the biocompatibility [1, 8-14]. There are several disadvantages to these methods. A time line of immune response is hard to determine unless many animals are used because

only one data point can be obtained per animal. Using many mice allows for more error associated with animal variability.

To circumvent these problems, we propose an alternate method of monitoring immune response. *In vivo* bioluminescence imaging allows measurements of immune response to be acquired real time. Transgenic mice expressing the proximal 5' human immunodeficiency virus long terminal repeat, a known Nuclear Factor-kappa Beta (NF-kB) dependent promoter sequence, are used. NF-kB is a transcription factor that plays a critical upstream role in coordinating the inflammatory and wound healing cascade. It initiates the transcription of many cytokines, chemokines, adhesion molecules, and proinflammatory genes [15-18]. When NF-kB binds to its promoter sequence to initiate transcription of immune response proteins, luciferase complementary DNA is also produced in the cell. Luciferase, in conjunction with its substrate, luciferin, catalyzes a bioluminescent reaction detectable by a sensitive charge coupled device camera. The amount of light (photons/sec) detected by the camera is therefore indicative of NF-kB activity, which is highly involved in regulating the immune response. These techniques allow unlimited measurements of biocompatibility to be made real time. Acquiring information from the same mouse repeatedly to construct a time line of immune response allows each new data point an accurate reference to the last, instead of relying on data points acquired from different animals. This is in part made possible because each mouse can be used as its own control. The requirement for fewer animals reduces the reliance on statistical analysis and increases the importance of real time data. Collected data can reveal important information about the immune response time course.

Materials and Methods

Capsule Fabrication

Capsules are fabricated using an air-stripping apparatus. Isolated Islets of Langerhans are mixed with the alginate polyanion solution. When the anion drops react with the cation solution to form the capsule walls, the islets remain sequestered inside. Alginate polyanion drops are sheared with air from the nozzle tip that funnels it. The diameters of the droplets are largely regulated by the controlled airflow around the nozzle tip. The nozzle tip diameter is also important in determining the polyanion drop size.

In order to form the capsule walls, the anion drops are washed in a polycation bath of $CaCl_2$. The alginate polyanion is comprised of guluronic and mannuronic acid residues which forms a hydrogel when cross linked with divalent cations, for example calcium [48]. The reaction time dictates wall thickness. In order to ensure consistent reaction times for all anion drops, a novel reactor is used. This reactor is a loop through which the $CaCl_2$ solution continuously flows. Once the capsule exits the reactor, it settles into a buffer solution, ending the gelling reaction (figure 4).

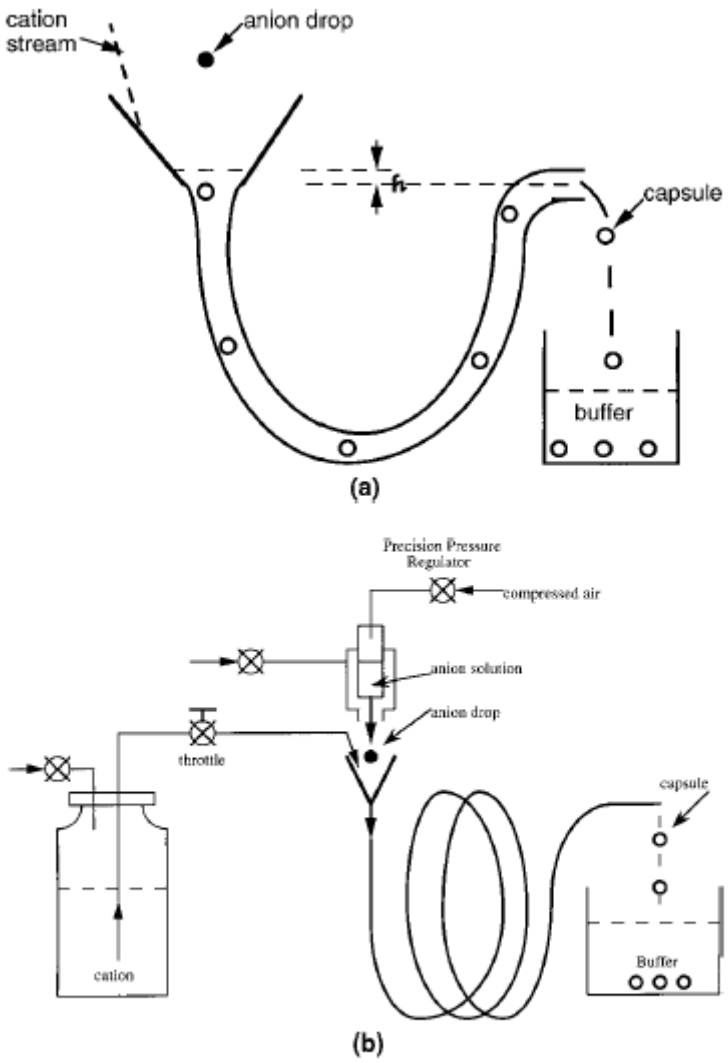

Figure 2. (a) The single-loop capsule reactor, and (b) the complete experimental layout for generating uniform capsules with a multiloop reactor.

Figure 4. Schematic of polyanion drop generator and cation solution reactor [49].

The flow rate and reactor length, which determine reaction time, remain constant. This allows equal reaction times for each capsule.

Once wall construction is complete, the capsules are washed in poly(methylene-co-guanidine)hydrochloride (PMCG) to create the capsule semi-permeable membrane.

This step is critical for determining pore size and therefore what particle sizes are allowed to diffuse through the capsule wall. Next the capsules are coated in another polyanion solution followed by one more $CaCl_2$ wash. This forms a final coating while eliminating superfluous positive ions from the PMCG solution.

These reactions produce capsules, which in this experiment are a transplant group. Another transplantation group is the non-coated capsule group. These non-coated capsules are the same size as the original capsules, but lack the final polyanion/$CaCl_2$ coating. They are used as a positive control because exposed positive ions are not biocompatible. The PMCG has been shown to induce TNF-α production and necrosis of monocytes [8]. To validate the efficacy of the imaging systems ability to discern between varying amounts immune response, a positive control is necessary.

The final transplantation group is the bead group. Beads are made by replacing the capsules into the drop generator with alginate. Larger capsules are formed when drops are sheared into the polycation reactor, forming larger beads that sequester an average of 2.5 capsules within. The capsules and beads have the same wall composition, and the difference is their diameters. The non-coated and normal capsule have an average diameter of .8mm. The beads have an average diameter of 1.4mm.

Bead dimensions allow more distance between the mouse and the encapsulated islets and leached debris. The beads also distance the only potentially toxic substance used in capsule fabrication, PMCG, from the mouse biological medium. The bead group was chosen to explore the potential negative effects of increased capsule diameter on NF-kB activity amidst the theoretical benefits of distancing the foreign cells and potentially toxic substances from the mouse biological medium.

Surgical Transplantation

The dorsal-cervical fat is chosen as the site of implantation for several reasons. Transplantation into the peritoneum does not allow for even distribution. Free-floating capsules are much less likely to show capsular overgrowth, and are easier to recover than those embedded in the peritoneal lining. Implantation into the fat pad reduces that selection bias. When capsules are transplanted into epididymal fat pads, capsules stay localized. Experiments have shown that pericapsular reactions are uniform throughout the pad [10, 50]. In addition, initial bioluminescent studies for this experiment show low basal NF-kB activity in the dorsal-cervical region relative to other fat pad locations closer to organs with elevated basal NF-kB activity.

The mice are first anesthetized with a 5mg/ml solution of nembutal. Each mouse is injected with 1/100 the mouse weight in milliliters. For example, a 30g mouse is injected with a .3mL dose of the 5mg/ml nembutol/saline solution. Prior to intra-peritoneal injection, the mice are anesthetized with gaseous isofluorane to render them motionless during IP injection. The injection of nembutal will anesthetize the mice for approximately 30-35 minutes.

Once anesthetized, each mouse is shaved along the dorsal-cervical fat pad, starting just below the base of the skull approximately 1/3 the length of the back. Then the mouse limbs are restrained to the surgical table. Once restrained, the shaved skin is swabbed with alcohol and the entire mouse is covered in swabbed plastic Saran wrap to help prevent infection.

Using tweezers and surgical scissors, an incision is made, first in the Saran wrap, and then the skin. Care is used to ensure the cut is made superficially into the skin to

prevent piercing of the membranous tissue beneath. Once the epidermis is incised, another incision is made in the thin membrane that separates the skin from the fat pad that lies beneath. Once this membrane is cut, the fat pad is exposed. The fat pad consists of sheaths of fat, between which space can be formed. Using surgical tweezer tips, the fat is probed until a separation in the sheaths of fat is located. Using the same tweezers, the sheaths are separated and held apart, and kept moist with sterile saline as necessary. This forms a small pocket into which capsules can be transplanted.

Capsules are most easily transported in solution. To provide adequate nourishment for the islets, the capsules are stored in a fetal bovine serum solution. Prior to transplantation, the capsules are transferred to a sterile saline solution and split into aliquots. Aliquots of different capsule types are normalized to surface area. During transplantation, the aliquots are siphoned into a pipette tip, and time (several minutes) is given to allow the capsules to gather at the bottom of the pipette tip. The pocket into which the capsules will be transplanted does not allow a volume of more than a drop or two of solution depending on mouse size. To avoid overflow, all capsules must be transferred in one to two drops of saline solution only.

Once the capsules are transferred, a single suture is tied joining the incised membrane that separates the skin and fatty tissue of the dorsal-cervical fat pad. Several sutures (as required) are then tied joining the incised epidermis. Each mouse is wrapped in gauze for warmth while the effects of the nembutol dissipate.

Image Acquisition

Each mouse is briefly anesthetized with gaseous isofluorane to render the mice immobile for several seconds for intra-peritoneal injection of a 5mg/ml solution of nembutal. Each is injected with 1/100 of their respective body weight, in milliliters. For example, a 30g mouse is injected with .3mL of the 5mg/ml nembutal in saline solution. Once anesthetized, mice are shaved over the dorsal-cervical fat pad from which photon counts will be acquired. Then each mouse in injected with a 15mg/ml solution of D-luciferin potassium salt in H_2O (Biosynth International Inc., Naperville, IL). Dosage is dependent on weight as is the nembutol, and the injection in intra-peritoneal.

After luciferin injection, each mouse is placed stomach down on a pad constructed specifically of dark material for imaging. Mice are immobilized on the pad by strapping their limbs to the surface. Each mouse head is immobilized by placing pins on either side of the head and in front of each ear. This restrains the head from shifting during involuntary reflex arcs and muscle spasms while anesthetized. Mouse movement must be kept to a minimum because exposure time is three minutes. Maximum bioluminescence from the bioluminescent reaction will occur at different times for each mouse. In addition, it will occur at different times for the same mouse on different days depending on several factors such as metabolism and subtle differences in injection location. Therefore, images acquired using 3-minute exposure times are taken consecutively for approximately 30 minutes.

Images are acquired using a XENOGEN IVIS 100 Imaging System and a charge coupled device camera (Spectral Instruments Inc.). Once images are acquired, the accompanying software (Living Image 2.2) is used to define a region on the image from

which photons are counted. The same area circle, large enough to encompass the dorsal-cervical region, was used for every image of every mouse. Because consecutive 3-minute exposures are taken over 30 minutes, there are approximately 10 resulting images per mouse per day. Each image was taken using a high resolution binning of 4, field of view 25, and all images were automatically background subtracted, flat-fielded, and cosmic. The image that renders the highest photon count per mouse is used for that day's data point. These intermediary steps are essential because they offer a standard method by which maximum bioluminescence can be obtained under variable conditions.

Luciferase Assay

A luciferase assay is performed to correlate photons detected by the camera to *in vivo* histology of the mouse dorsal-cervical fat pad. Small adipose tissue samples, approximately .006g, are selected from three mice, one transplanted with capsules, another transplanted with capsules lacking a final coating, and a last transplanted with the larger beads (a larger capsule, approximately 1.4mm in diameter, sequestering 2-4 capsules of standard diameter, approximately .8mm in diameter). Samples were taken approximately 7 weeks post-transplantation.

Each tissue sample is placed in a solution of 1x PBS solution for rinsing. Each sample is gently blotted dry and weighed. A diluted Reporter Lysis Buffer (Promega Corp., Madison, WI) is added to each sample. Cells containing the luciferase must be lysed. For every 1ug tissue, 1uL lysis buffer is added. For each sample, only small amounts of buffer are added at first. Fatty tissue is difficult for the buffer to break down and requires manual methods of digestion. In this case, a small aliquot of lysis buffer is

added to each sample in an epindorph tube, and the tissue then cut with small surgical scissors into smaller pieces that enables the buffer to digest more completely and quickly. Adding all the buffer at once would hamper this process because there would be too much solution in the tube to effectively cut the tissue. The remaining buffer is added to each sample after cutting and incubation so the ratio of tissue to buffer is consistent for each sample. Results are normalized per gram tissue weight.

Each sample is incubated in the buffer for approximately one half hour. At this point, the tissue is soft and easily broken, but not completely broken down. Each sample is then placed in a thick test tube used for grinding. Each sample is ground with a pestle instrument manufactured to fit the diameter of the epindorph tube until the tissue is "dissolved" in the lysis buffer. A small aliquot of the resulting solution is taken from each sample and placed in epindorph tubes. They are shaken vigorously and then spun for 4 minutes. The spinning separates the tissue proteins from the luciferase protein. From each spun sample, a small consistent aliquot of 20uL is acquired and added to 50uL lysate solution (Promega Corp., Madison, WI), which is placed in a Luminometer for luciferase protein detection.

The lysis buffer, with the dissolved tissue, added to the lysate solution is placed in a special tube deigned for use with the Monolight 3010 Luminometer. The luciferase catalyzes the bioluminescent reaction with the lysate and the resulting light emittance is amplified and detected by a high sensitivity, low noise photomultiplier. The number of photons emitted during the reaction is indirectly related to the luciferase content in that tissue sample. The resulting units are RLUs, or relative light units.

H and E Stain

An H and E stain was performed to visualize fibrosis surrounding different types of capsules. Three tissue samples are extracted, approximately 7 weeks post-transplantation, from the same three mice used for the luciferase assay, one transplanted with capsules, another transplanted with capsules lacking a final coating, and a last transplanted with the larger beads.

Care is taken to ensure that capsules are embedded in the extracted samples. Each sample is suspended in a formulin fixative, provided by the Pathology Core, Vanderbilt University.

Once suspended in the formulin fixative, the samples are given to the Pathology Core, Vanderbilt University for embedding in paraffin blocks. Slices from each block are cut to make slides, and those slides containing cross-sections of the polymer-based capsules are treated with an H and E stain to mark immune response proteins surrounding the capsule.

Trouble Shooting

It is important to ensure that the variance in the results is due to inherent bio-variance and not due to inconsistencies in the experimental procedure. Various troubleshooting projects were conducted to exclude any additional error that may be contributed by the camera, mouse physiology other than NF-kB activation, tissue specificity of the NF-kB transcription factor, effects of repeated shaving (not including surgery), and substrate concentration consistency.

Camera Consistency

In order to exclude any variance in photon count acquisition by the CCD camera, small glass beads (mb-Microtec, Switzerland) of constant luminescence are used for calibration. Each glass droplet, dimensions .65 x 2.5mm, luminesce at constant intensity at 550 +/- 10nm.

Twenty beads are imaged several times daily over a period of five days to determine both long and short term photon count regularity. The average and standard deviation are calculated from the images for each bead. The percent standard deviation of the average is calculated for each bead (st. dev. / average), and the twenty separate percents are averaged to obtain a final average of 4.4%.

It is unknown whether this 4.4% reflects the camera's ability to measure a constant light source consistently, or whether it reflects the glass bead's ability to luminesce at constant intensity. Regardless, 4.4% is much smaller a ratio than the standard deviation to average ratio of 38.5% for the baseline measurements for each mouse, an almost 9-fold difference.

Tissue Specificity of the NF-kB Transcription Factor

The NF-kB transcription factor is tissue specific. It behaves differently depending on the tissue. For example, basal NF-kB activity is higher in some tissues than in others. In order to determine if there is a marked increase of basal NF-kB variability at the site of transplantation compared to elsewhere in the mouse model, a comparison was made against the nose. The nose was chosen for its accessibility in the images, and its high basal level of NF-kB activation, in contrast to the fat pad. Other parts of the mouse

anatomy available are the ears, which are too close to the dorsal-cervical area, the paws, which are often covered due to the mouse limb restraints, and the tail, which is often not in the image frame, and twitches under anesthesia. The nose is the easiest to isolate.

Data from six mice imaged five times over two weeks is used. The images are procured and integrated intensities calculated in the same manner described in the Materials and Methods section outlining Image Acquisition. For both anatomical regions, both the average and the standard deviations are calculated for each mouse using the data obtained from the five imaging sessions. For each mouse, the ratio of standard deviation to the average (st. dev. / average) is calculated to determine what percent of the average the standard deviation represents. Six mice results in six percentages. The average and standard deviation of those percentages are calculated for each anatomical region. The nose data results in an average of 33 +/- 16%, and the fat pad data results in a ratio of 42 +/- 10%. These are statistically insignificant, and no conclusion can be easily drawn about the variability of NF-kB activation in these two different tissue samples.

A possible explanation for the larger percent error from the fat pad data is the difference in size of the region measurements. The region measurements for the nose cover a much smaller area of the mouse than those for the fat pad. The slightest variations, such as mouse movement, physiological variations in the mice, could be augmented when looking at those effects over a larger surface area. It is logical that the fat pad presents a higher ratio.

Shaving Effects

Another possible source of NF-kB activation, other than trauma from surgery and immune response to transplant materials is shaving of the skin over the dorsal-cervical fat pad. Prior to imaging, each mouse is shaved as needed because fur can mask bioluminescent signals. A study was conducted using two mice to determine any adverse effects.

Three baseline measurements of the dorsal-cervical region are taken prior to shaving. Prior to the fourth imaging session, each mouse is shaved. Subsequent imaging of the dorsal-cervical fat pad is preceded with a shave, regardless of its necessity to remove hair; mice require trimming approximately once every one to two weeks. For this study, it is important to conduct shaving prior to each imaging session because the effects of long-term shaving are to be determined.

Results indicate an average increase in light emmitance of 41% without fur. This increase is expected. However, the purpose of this experiment is to compare the fourth imaging session shave day data (before any irritation and subsequent NF-kB activation from shaving has a chance to occur) to data acquired during the fifth, sixth, and seventh imaging sessions (presumably irritation increases bioluminescence if shaving instigates irritation). According to the results, no significant increases in luminescence occurs post shave day (data not shown).

Luciferin Saturation Studies

A potential area of bioluminescent variability is substrate concentration. Doses of luciferin are injected into the peritoneal cavity of the mice prior to placement in the

imaging chamber. There are many factors that can vary the amount of substrate reaching immune response cells in the dorsal-cervical fat pad such as biodistribution, cellular uptake, and enzyme kinetics. Because of these factors, it is easy for resulting bioluminescence to be proportional to the amount of injected substrate instead of proportional to the amount of endogenously produced intracellular luciferase enzyme.

To effectively exclude potential substrate problems such as inconsistent dilutions, freeze/thaw freezers that may slightly thaw the luciferin solution and reduce potency, studies to determine saturation thresholds are conducted. Two mice are used for this experiment. It is important to use mice that have already undergone surgery because NF-kB activation will increase over basal levels, and more luciferase complementary DNA will be present.

For this study, two mice are injected with single, double, and triple doses of luciferin during the course of one day, with at least 5 hours separation. Luciferin concentration is the same as described in the Materials and Methods section outlining Image Acquisition. It is important to conduct this study within a period during which it can be assumed significant levels of immune response have not changed. For each mouse, the standard deviation of the results for all three dosages is less than the standard deviation of baseline measurements for each mouse (data not shown). This indicates that the substrate concentrations are at or near appropriate levels to overcome any saturation obstacles such as enzyme kinetics, biodistribution, and cellular uptake. To compare varying levels of bioluminescence, which is assumed to be indicative of immune response, it is important to ensure that limiting reagent is not dependent on levels of injected luciferin, but rather on levels of endogenous luciferase.

Results

As previously mentioned in the Materials and Methods section outlining Image Acquisition, images were acquired using consecutive three-minute exposures for approximately 30 minutes. Maximum bioluminescence occurs at different times for each mouse, and at different times for the same mouse on different days depending on metabolism, subtle differences in injection location, cellular uptake, and enzyme kinetics (figure 5).

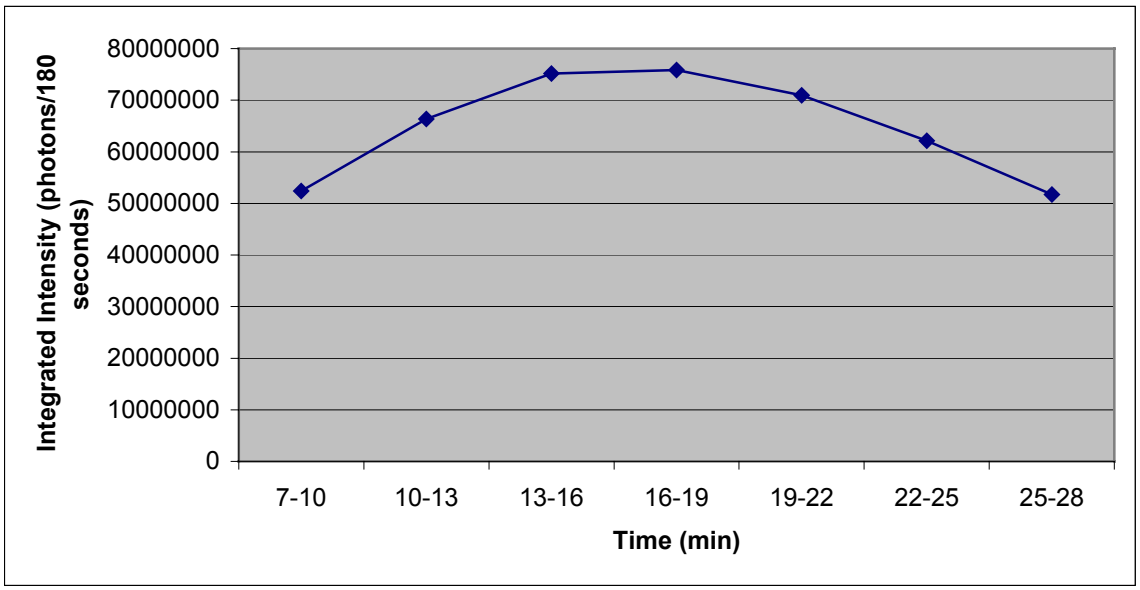

Figure 5. Graph of bioluminescent reaction time course after luciferin injection for one mouse.

This inherent variability changes the characteristics of the above graph in figure 4. The maximum data point per mouse (16-19 minutes for this mouse on this imaging day) is used because it is the most indicative of the total amount of luciferase complimentary DNA present at the site of implantation. The maximum point is theoretically consistent over multiple image acquisition sessions. Care was taken to ensure that the limiting

reagent in this bioluminescent reaction was the luciferase complementary DNA and not the injected luciferin, as described in the Trouble Shooting section outlining Luciferin Saturation Studies.

To determine statistically significant differences between transplant groups per imaging session, and to compare total bioluminescent activity between transplant groups over a period of six weeks, normalization procedures were required. Between three and five baseline measurements of the dorsal-cervical fat pad were obtained before surgical procedures for each mouse. These measurements were averaged and represent basal NF-kB activity for each fat pad. This average was used as a base for which every subsequent post-surgical measurement could be inferred as a percent increase over basal NF-kB activity. This process standardizes varying degrees of basal NF-kB activity across the mice.

Four rounds of surgeries were conducted during the course of the experiment. To compare total bioluminescent activity between transplant groups over all six weeks, it was important to normalize the time-axis as two of the four transplantations were monitored for approximately four weeks. This required multiplying those transplantations by a conversion factor obtained from the capsule group from the first transplantation, which was monitored over the entire six weeks. An assumption must be made that the transplant groups in the two transplantations monitored for only 4 weeks would behave similarly to the capsule group in the first.

Time axis normalization and normalization of transplant group data was calculated with respect to the capsule group in each of their respective rounds of surgery for several reasons. First, mice were transplanted with capsules in all four rounds of

surgery. Second, as described in the Materials and Methods section outlining capsule fabrication, fabrication techniques allow for very high reproducibility. The air-stripping apparatus allows a high degree of polyanion drop uniformity. The chemical reactor that generates the continuous flow of $CaCl_2$ solution allows reaction times to be controlled within a few percentage points, which is important because reaction times between the alginate drop and the $CaCl_2$ solution dictate membrane thickness. In addition, collection of polyanion drops in a beaker of polycation solution allows for sedimentation and varying reaction times between the first anion drop to fall compared to the last. Both of these phenomenons can result in heterogeneity of wall thickness. The chemical reactor ensures uniform capsule exposure to the cation solution. These procedures aid in producing capsules under identical conditions [49, 51]. It is for these reasons that every transplant group was normalized to the capsule group in that round of surgery. For example, the bead group from the second transplantation was normalized to the capsule group from the second transplantation; hence, the normalized area under the curve for the capsule group is 1 for each surgery. Normalized results from each transplantation were then averaged (figure 6).

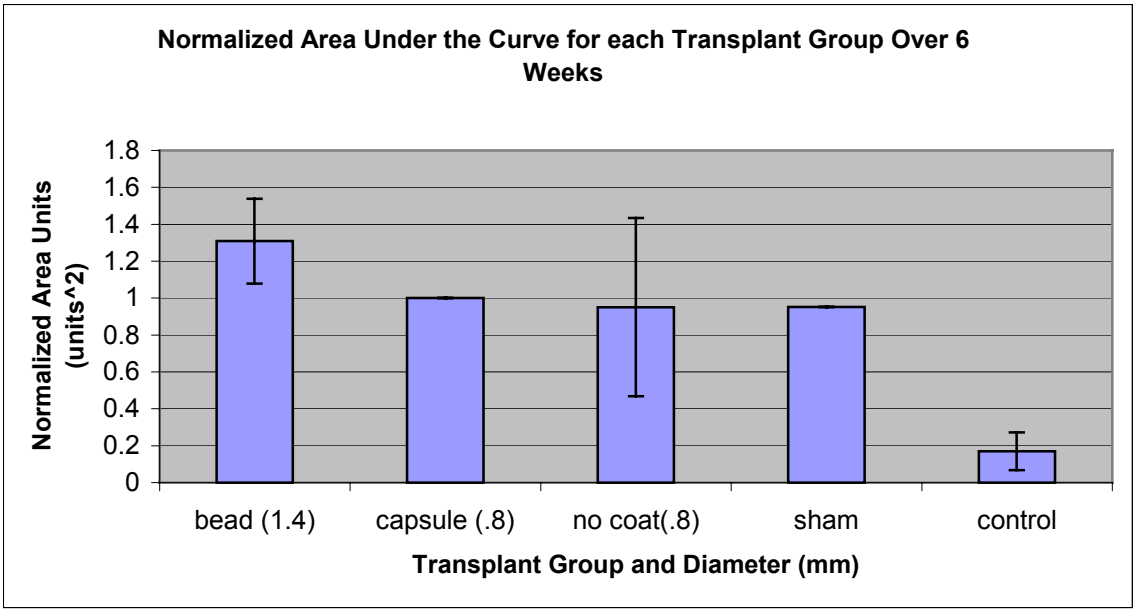

Figure 6. Bar graph of normalized area under the curve for each transplant group. All transplant groups are normalized to the capsule group, which equals 1. The numbers in parenthesis are diameters (mm). Error bars represent standard error of the mean. There is no error for the capsule group because the area under the curve is normalized to 1 in all transplantations. There is no error for the sham group because they are monitored in only one round of transplantation.

It can be inferred from the figure 5 that there is little difference in NF-kB activity over a six-week period between the capsule, no coat, and sham groups. Activity for the no coat and sham group was suppressed approximately 5% below capsule NF-kB activity. However, NF-kB activity resulting from bead transplantation was elevated approximately 31% over capsule activity, statistically significant relative to the capsule transplant group. As expected, control group activity was largely suppressed, approximately 83% below capsule activity.

The normalized time line of NF-kB activity for each transplant group is presented in the following graphs (figure 7-11).

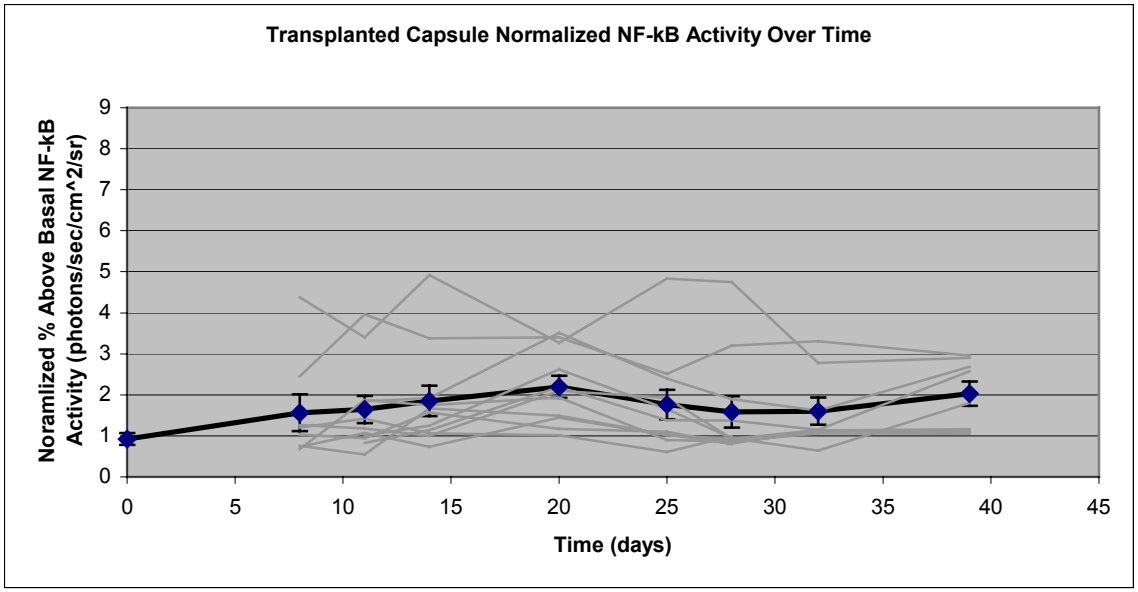

Figure 7. Graph of normalized NF-kB activity for mice transplanted with capsules. Day 0 is surgery day, and is represented by the average of all pre-operative baseline measurements for all mice in the group. Error bars represent Standard Error of the Mean. N = 11.

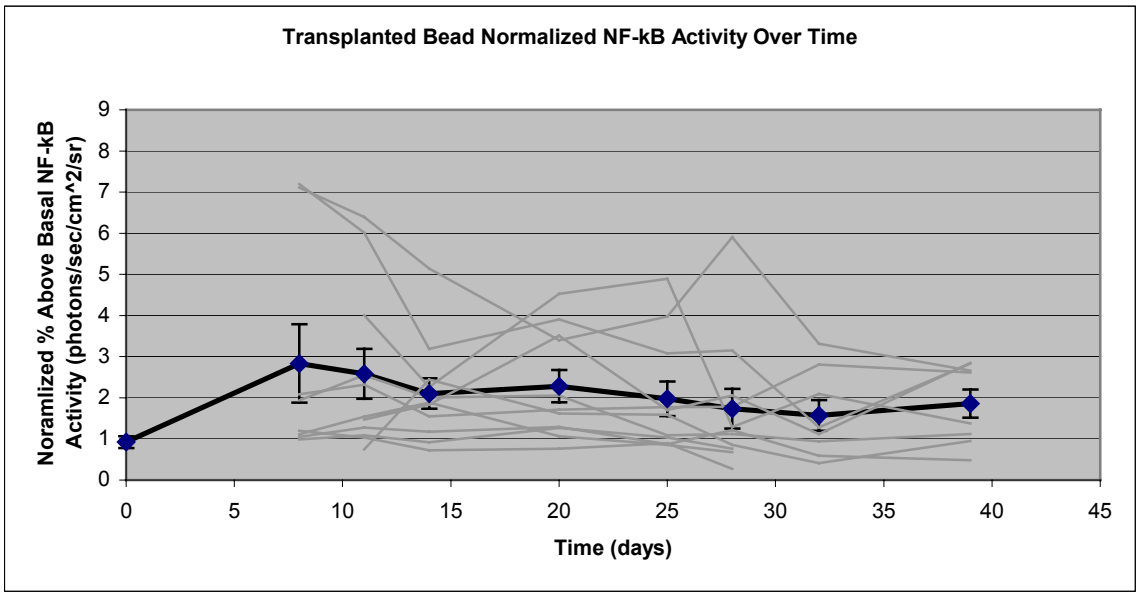

Figure 8. Graph of normalized NF-kB activity for mice transplanted with beads. Day 0 is surgery day, and is represented by the average of all pre-operative baseline measurements for all mice in the group. Error bars represent Standard Error of the Mean. N = 11.

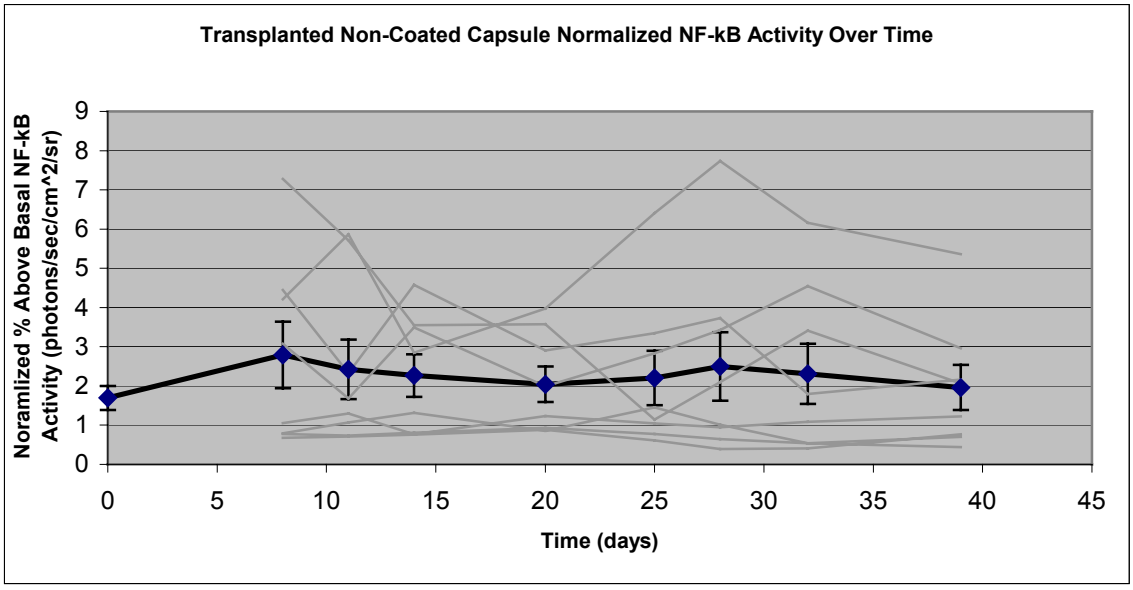

Figure 9. Graph of normalized NF-kB activity for mice transplanted with non-coated capsules. Day 0 is surgery day, and is represented by the average of all pre-operative baseline measurements for all mice in the group. Error bars represent Standard Error of the Mean. N = 8.

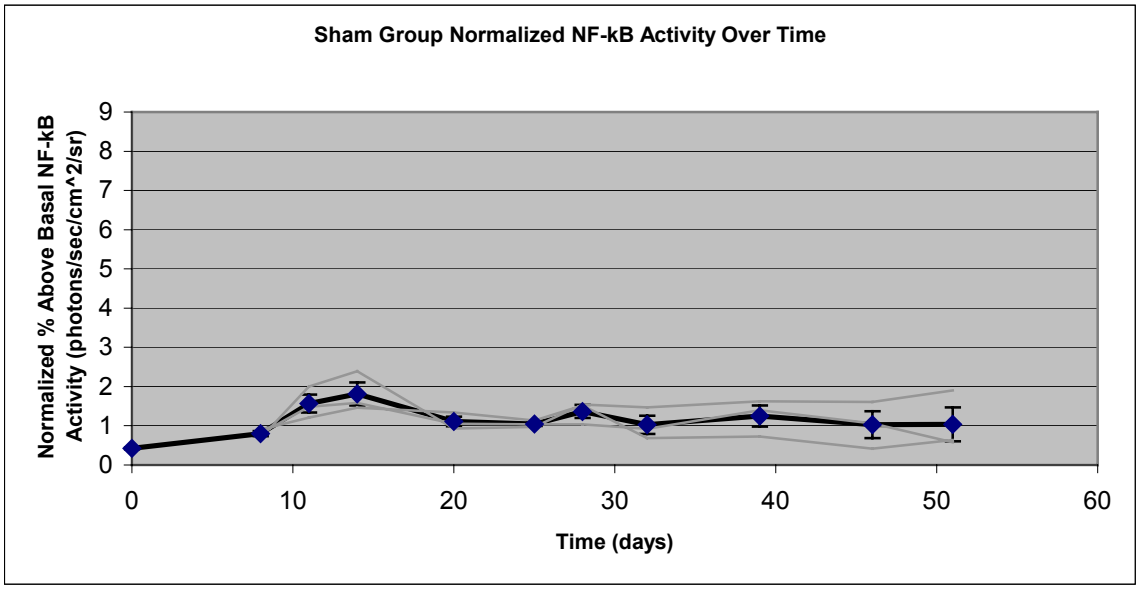

Figure 10. Graph of normalized NF-kB activity for sham surgery mice. Day 0 is surgery day, and is represented by the average of all pre-operative baseline measurements for all mice in the group. Error bars represent Standard Error of the Mean. N = 3.

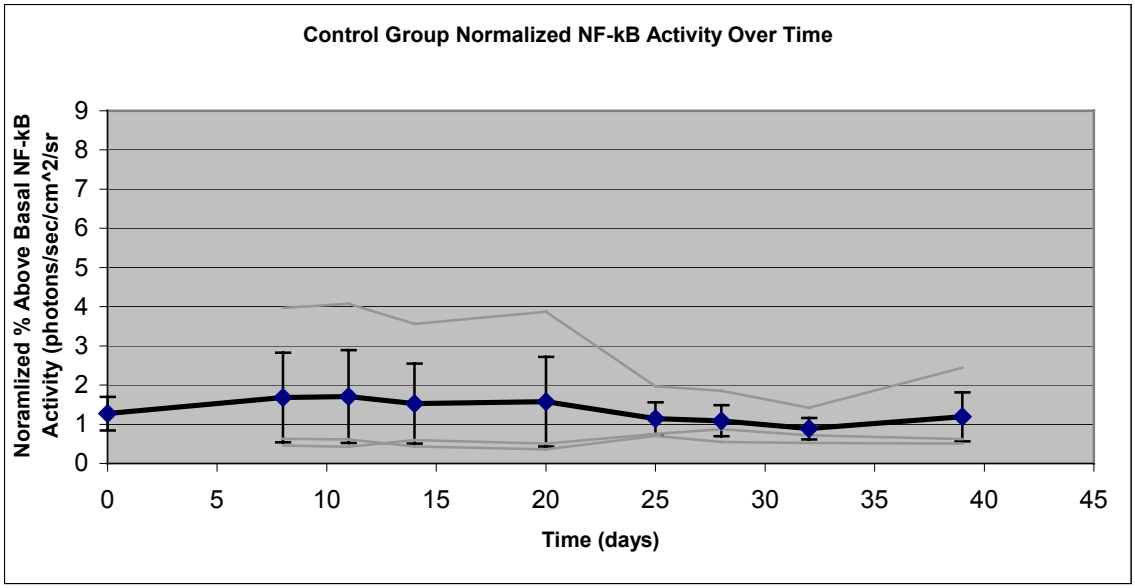

Figure 11. Graph of NF-kB activity for control mice. Day 0 is surgery day for the mice in other groups, and is represented by the average of all baseline measurements for the mice in the control group. Error bard represent Standard Error of the Mean. N = 3.

Statistical analyses reveal no statistically significant differences between groups per imaging session. The only point at which there is a statistically significant difference between the medians of transplant groups is between the bead and sham groups, 8 days post surgery. The following table shows Mann-Whitney P values for comparisons calculated between each group (Table 1).

Table 1. Table of Mann-Whitney P values for comparisons between groups. P<.05 is statistically significant and marked in bold with asterisks. Cells marked with a Not Available indicate that sample numbers are too small to perform the Mann-Whitney Test. The Sham vs. Control group is not included because sample numbers are too small for all dates. X-axis is days post surgery.

	8 days	11 days	14 days	17 days	20 days	25 days	28 days	32 days	39 days
Bead vs. Capsule	0.279	0.189	0.393	0.841	0.948	0.948	1	0.721	0.645
	(16)	(22)	(22)	(10)	(22)	(22)	(22)	(16)	(16)
Bead vs. No Coat	0.721	0.591	0.967	0.73	0.591	0.901	0.65	0.878	0.798
	(16)	(19)	(19)	(9)	(19)	(19)	(19)	(16)	(16)
Bead vs. Sham	**0.012**	0.876	0.876	NA	0.119	0.533	0.876	0.63	0.63
	(11)	(14)	(14)		(14)	(14)	(14)	(11)	(11)
Bead vs. Control	0.279	0.276	0.35	NA	0.276	0.213	0.64	0.497	0.279
	(11)	(14)	(14)		(14)	(14)	(14)	(11)	(11)
Capsule vs. No Coat	0.442	0.65	0.71	0.556	0.65	0.773	0.483	1	0.645
	(16)	(19)	(19)	(9)	(19)	(19)	(19)	(16)	(16)
Capsule vs. Sham	0.376	0.436	0.64	NA	0.062	0.436	0.35	0.376	0.279
	(11)	(14)	(14)		(14)	(14)	(14)	(11)	(11)
Capsule vs. Control	0.376	0.533	0.35	NA	0.436	0.35	0.436	0.279	0.133
	(11)	(14)	(14)		(14)	(14)	(14)	(11)	(11)
No Coat vs. Sham	0.376	0.921	1	NA	0.776	0.376	1	0.776	0.776
	(11)	(11)	(11)		(11)	(11)	(11)	(11)	(11)
No Coat vs. Control	0.194	0.279	0.279	NA	0.376	0.376	0.376	0.497	0.497
	(11)	(11)	(11)		(11)	(11)	(11)	(11)	(11)

To ensure that data obtained from imaging is indicative of varying quantities of luciferase complementary DNA, a luciferase assay was performed on three mice, one transplanted with beads, another with capsules, and the last with non-coated capsules. The following diagram displays the raw integrated intensities for each mouse at the time

of assay and the corresponding value of relative light units projected by the spectrometer (figure 12-13).

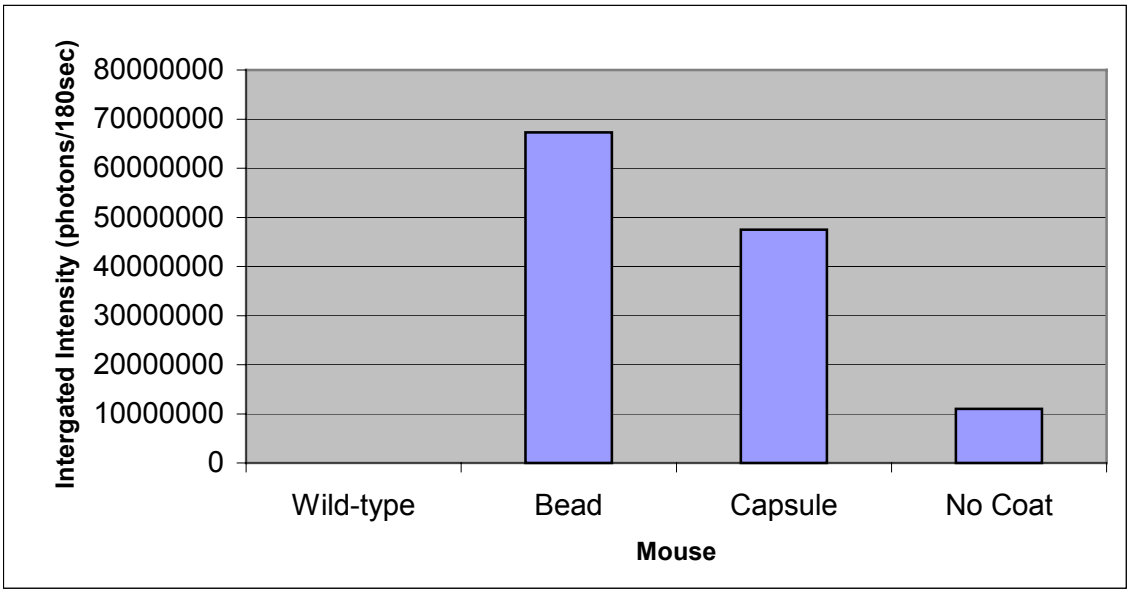

Figure 12. Graph of integrated intensities from four mice the day before luciferase assay.

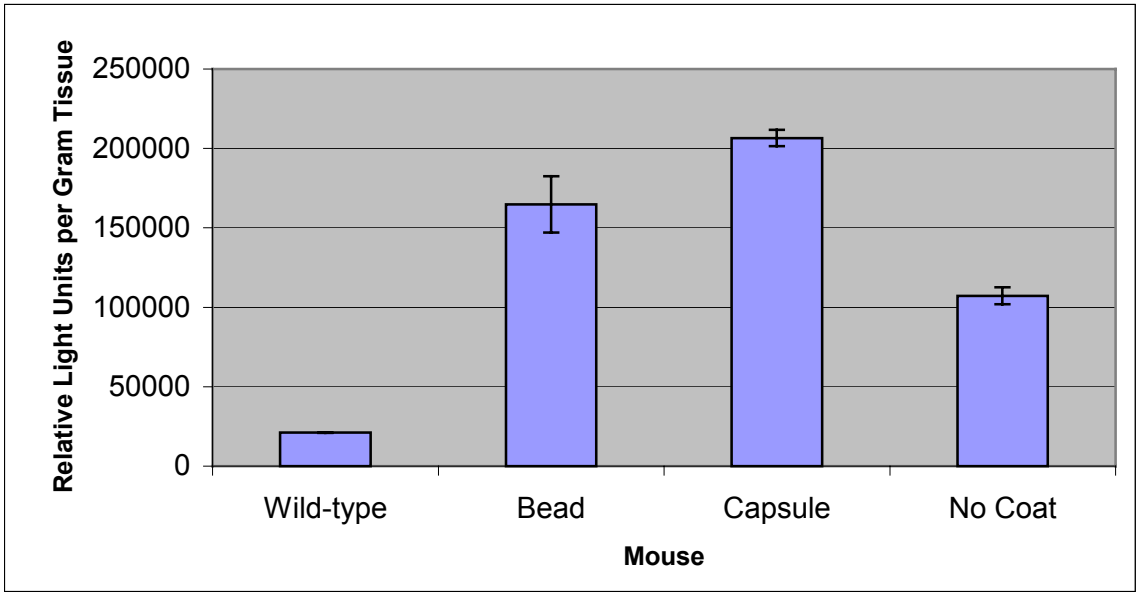

Figure 13. Results of luciferase assay from mice transplanted with capsules, beads, and uncoated capsules. Data is normalized per gram tissue weight.

The no coat mouse exhibited approximately a quarter to a sixth the integrated intensity of the capsule and bead mice, respectively. Accordingly, the luciferase assay data obtained shows the no coat mouse tissue sample contained approximately half to three fifths the luciferase quantity per gram tissue of the capsule and bead mice, respectively. All three transplant groups showed significantly greater amounts of luciferase than the wild type mouse.

In addition to the luciferase assay, retrieved capsules still embedded in the dorsal-cervical fat pad from the same three mice were extricated and embedded for H and E staining. Photographs of each cross section show a markedly higher congregation of immune response proteins surrounding the bead and capsule walls than the no coat walls (figure 14-16).

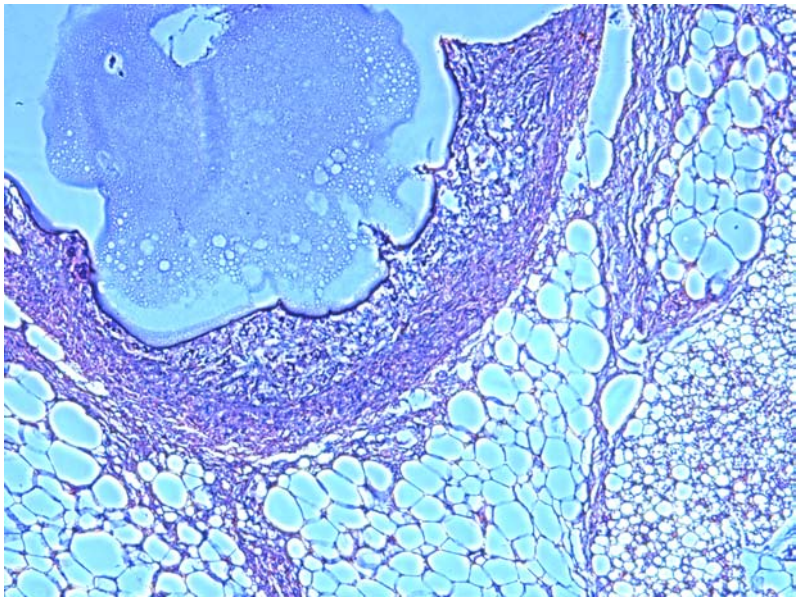

Figure 14. Image of H and E stained cross section of excised bead from dorsal-cervical fat pad. Aqua cells are adipose tissue. Purple grain surrounding bead wall is fibrosis.

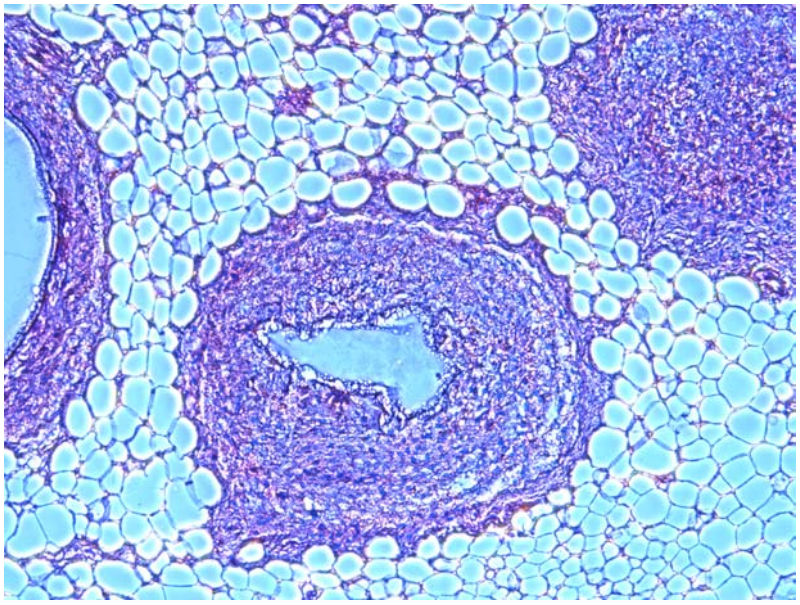

Figure 15. Image of H and E stained cross section of excised capsule from dorsal-cervical fat pad. Purple grain surrounding capsule wall is fibrosis.

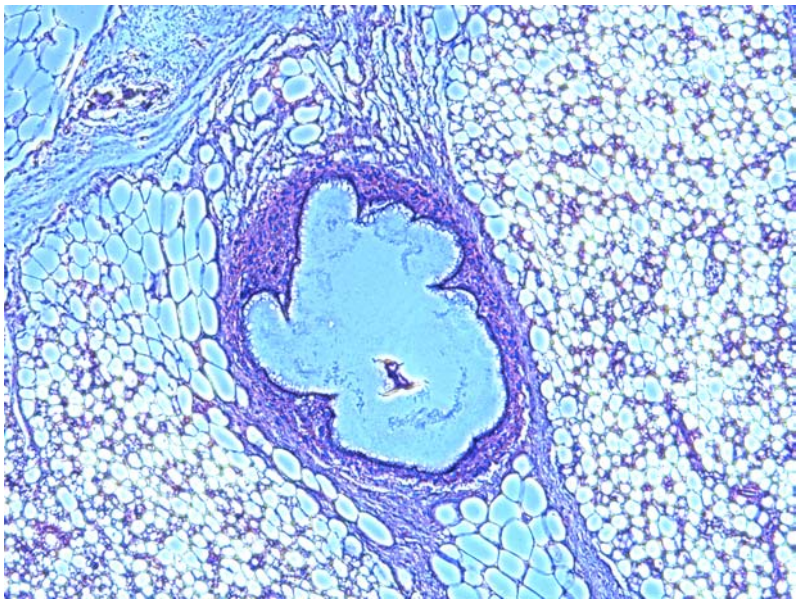

Figure 16. Image of Hand E stained cross section of excised non-coated capsule from the no coat transplant group dorsal-cervical fat pad. Purple grain surrounding capsule wall is fibrosis, of which there is considerably less compared to excised beads and capsules with final coating.

It is important to note that these three mice are not necessarily representative of their perspective transplant group, but rather they verify the correlation between bioluminescent intensities acquired from the camera and mouse histology.

Discussion

Results from this experiment indicate that this imaging modality can be a proficient methodology for monitoring immune response real time and *in vivo* using the NF-kB transcription factor as a bioluminescent marker. It is capable of determining statistically significant differences between pre and postoperative data points per mouse, as well as differences in NF-kB activity between transplant groups over a six-week period of time.

Five transplant groups were monitored over four rounds of surgeries, a capsule, no coat, bead, sham, and control group. The capsule group is those mice implanted with standard uniform capsules approximately .8mm in diameter. The non-coated capsules are capsules of the same size, but lacking a final biological coating to be used as a positive control, as described in the Materials and Methods section outlining capsule fabrication. The control group consists of mice that did not undergo surgery, monitored for the effects of repeated nembutol and luciferin injections, and used as a negative control. The bead group is essentially identical to the capsule group in surface composition, but has an average diameter of 1.4mm. The sham group consists of mice that experienced surgical procedures, but no implant was left in the fat pad, allowing us to monitor surgical effects on NF-kB activity. These transplant groups were chosen to allow comparisons between both the capsule wall composition and size parameters to be made.

The sham transplant group time line of NF-kB activity shows an initial peak shortly after surgery, and then a slow decrease in NF-kB activity over several weeks back to basal levels. The bead, capsule, and no coat groups show similar responses, indicating that they, too, experienced initial increases in NF-kB activity due to surgical procedures. Both the no coat and sham groups show only a 5% decrease in NF-kB activity compared to the capsule group over six weeks. Because the normalized area under the curve for the capsule group is close to the sham surgery group, host immune response to the capsules is negligible compared to the trauma of surgery. This is potentially encouraging news for the success of encapsulated islets.

The same conclusion can be drawn about the no coat group. This is particularly interesting because even those capsules fabricated for use as a positive control demonstrate a degree of immune response still masked by the traumatic effects of surgical procedures. Within the variables modified in the production of capsules, the biocompatibility parameter has negligible effects on host NF-kB activity compared to surgical procedures.

The bead group shows a 31% increase in NF-kB activity over the capsule group and the sham group, indicating that the size parameter effects NF-kB activity in excess of the effects of surgical procedures over a six-week period. These results support findings by Robitaille et al. who found that larger capsules elicit a greater immune response when normalized to surface area, although the capsules studied are smaller in scale than those used in this experiment [10]. Experiments conducted by Paul de Vos et al. concluded that capsules of an approximate .8mm diameter have a lower percentage of incomplete (islet protrudes from microcapsule) and defective (sequesters islet but with localized defects)

capsules than capsules of an approximate 1.4mm diameter [52]. However, these results are an indirect representation of biocompatibility and more a direct representation of the limits of their capsule fabrication techniques, as techniques, chemicals, reactions times, and equipment change from one lab to another. Care is taken in this experiment to not only normalize transplant materials to a constant surface area, but also to ensure that there are no discontinuities in the capsule walls. Several experiments have been conducted to determine the effects of capsule size on water activity, mechanical strength, transport behavior, porosity, in vitro insulin kinetics, and TNF-α permeability, but not *in vivo* biocompatibility studies directly [53, 54].

Although the exact mechanisms for the apparent effect of capsule size on biocompatibility are not clear, there are several theories. Because both the capsule and bead surfaces are similar in composition, and total transplanted surface areas are normalized before transplantation, both individual volume differences between the capsules and beads, and the total implant volume may have an effect. The transplanted beads occupy a larger total volume than the capsules. Larger volumes may provoke greater stress on neighboring cells. This may affect the rapidity of or ability to mount immune responses. Because capsules and beads are normalized to surface area, differences in the total number of implanted capsules (18) and beads (6) may also have an effect. Because the site of transplantation is close to the incision, it is more likely that larger implant volumes have no more an effect on inflammation than do the capsules, but rather a more negative effect on wound healing. The sham surgery indicates that wound healing does affect NF-kB activity.

This size dependence on capsule biocompatibility is particularly intriguing because of the PMCG distribution. It is an element used in capsule fabrication considered to elicit an immune response (T.G. Wang and Michael Haralson, private communication). Normalizing transplantation materials to surface area results in the transplantation of 18 capsules per mouse, and 6 beads per mouse. There are an average of 2.5 capsules sequestered within each bead. The process of bead formation does not require any additional PMCG. Therefore, not only is there less PMCG, on average, in those mice transplanted with beads, but they are also positioned further from the biological medium in the mouse. In addition to the PMCG, the mouse is also positioned further from the islets and its biological debris. These characteristics would lead one to hypothesize that the beads could be more biocompatible than the capsules, however, the effect of volume must be masking those effects, if any.

In conclusion, this imaging modality can be a practical methodology for monitoring immune response using the NF-kB transcription factor as a bioluminescent marker. Until now, biocompatibility measurements of the bioartifical pancreas have been made histologically, which allows only one data point to be acquired per mouse. Acquiring information from the same mouse repeatedly to construct a time line of immune response allows each new data point an accurate reference to the last, instead of relying on data points acquired from different animals. This is in part made possible because each mouse can be used as its own control. The requirement for fewer animals reduces the importance for statistical analysis and increases the importance for real time data. These advantages allow the following conclusions to be made about the efficacy of this imaging modality. It is sensitive enough to significantly differentiate between pre and

post operative data points per mouse, but not sensitive enough to discern differences between transplant groups per imaging session. However, it is capable of determining differences between transplant groups over extended periods of time. We found that the surgery itself and the size of transplant have more of an effect on capsule biocompatibility than does the wall composition parameter in this experiment. Neither the capsule nor the no coat groups are able to provoke a host immune response greater than that elicited by surgical procedures. Only beads with a greater diameter than the capsule and no coat groups are able to elicit host immune responses in excess of those triggered by surgical procedures.

CHAPTER III

FUTURE WORK

This imaging system, in conjunction with an NF-kB bioluminescent marker, is an effective means by which differences in biocompatibility due to capsule size can be scored over a period of time. However, the traumatic effects of surgery are an impediment to determining those differences, and even mask the effects of varying wall compositions on biocompatibility. Perhaps if the effects of surgical procedures could be minimized it would provide starker bioluminescent differences between capsules of varying sizes, present differences in NF-kB activity between capsules with varying wall compositions, and perhaps allow statistically significant differences per imaging session to surface.

Alternative surgical techniques that do not cause as much trauma may be useful. For example, a syringe with a small enough gauge needle to allow passage of the capsules could be used. Then, incisions would not be necessary, and the skin could be punctured far from the dorsal-cervical fat pad from which photon counts are acquired. This technique would deposit the capsules between the skin and the fat pad. Not having an incision in the skin would have to keep the capsules immobilized between the skin and the fat, since it would be difficult to make the fatty pockets into which the capsules were transplanted.

One potential problem with current techniques, as previously mentioned, is the overflow of capsules from the fatty pocket, from which one or two capsules could be

spilled during surgery. The proposed method may eliminate that variability. In addition, using the proposed technique would greatly reduce the chances of infection, and if infection did occur, it would not be at the area of photon count acquisition.

This imaging modality shows size dependant results. It would be interesting to explore those effects more thoroughly. Fabricated capsules of sequential sizes could be used and monitored for their effects on NF-kB activation. As mentioned in the discussion section, previous experiments have been conducted using capsules of sequential sizes, however, the results indirectly provide biocompatibility differences as a function of capsule integrity, not scored fibrosis.

Additionally, to assess the hypothesis that implant volumes may have an effect on NF-kB activity, it may be interesting to normalize the implants to volume instead of surface area. This would allow two parameters to be tested, capsules of homogenous volume and differing total implant volumes, but also capsules of heterogeneous volumes and a constant total implant volume, to determine the effects of varying numbers of implanted capsules on NF-kB activity.

It is also important to note that this imaging system may in fact be sensitive enough to determine differences between NF-kB activity elicited by all transplant groups if more than 3 minutes worth of data could be collected every 48 to 72 hours. Those three minutes represent .1% to .07% of the total time elapsed in 48 to 72 hours. If more data could be collected over those hours and then integrated, it may result in statistically significant differences between the transplant groups because a more accurate time course of NF-kB activity would be revealed. More data could allow trends in NF-kB

activity to surface that were somewhat obscured by the inherent noise associated with using live animals in this experiment, for example trauma due to surgery.

Another possible improvement that could be made to this experiment is to change the bioluminescent marker. Perhaps no matter how often measurements of NF-kB activity are made, the NF-kB transcription factor is important to too many cell signaling pathways involved in the inflammatory and wound healing cascades to determine statistically significant data. It may be beneficial to use this bioluminescent technology to mark the activity of other transcription factors, or perhaps others in conjunction with NF-kB. This may result in a needed reduction of background noise.

REFERENCES

1. de Vos P., d.H.B., Wolters G., Strubbe J., van Schilfgaarde R., *Improved Biocompatibility but Limited Graft Survival After Purification of Alginate for Microencapsulation of Pancreatic Islets.* Diabetologia, 1997. **40**: p. 262-270.

2. Shapiro J., L.J., Ryan E., Korbutt G., Toth E., Warnock G., Kneteman N., Rajotte R., *Islet Transplantation in Seven Patients with Type I Diabetes Mellitus Using a Glucocorticoid-Free Immunosuppressive Regimen.* The New England Journal of Medicine, 2000. **343**(4): p. 230-238.

3. Ricordi C., *Islet Transplantation: A Brave New World.* Diabetes, 2003. **52**: p. 1595-1603.

4. Scharp D., L.P., *Encapsulated Islet Implantation for the Treatment of Insulin-Requiring Diabetes*, in *Insulin-Free Times*. 2004.

5. Kenyon N., F.L., Lehmann R., Masetti M., Ranuncoli A., Chatzipetrou M., Iaria G., Han D., Wagner J., Ruiz P., Berho M., Inverardi L., Alejandro R., Mintz D., Kirk A., Harlan D., Burkley L., Ricordi C, *Long-term Survival and Function of Intrahepatic Islet Allografts in Baboons Treated with Humanized Anti-CD154.* Diabetes, 1999. **48**: p. 1473-1481.

6. Wang T., L.R., *Bioartificial Pancreas*, in *Principles of Tissue Engineering*, L.R. Lanza R., Vacant J., Editor, Academic Press: San Diego. p. 495-507.

7. Lim F., S.A., *Microencapsulated Islets as Bioartificial Endocrine Pancreas.* Science, 1980. **210**: p. 908-910.

8. Strand B., R.L., Veld P., Kulseng B., Rokstad A., Skjak-Braek G., Espevik T., *Poly-L-Lysine Induces Fibrosis on Alginate Microcapsules via the Induction of Cytokines.* Cell Transplantation, 2001. **10**: p. 263-275.

9. Wijsman J., A.P., Mazaheri R., Garcia B., Paul T., Vose J., O'Shea G., Stiller C., *Histological and Immunopathological Analysis of Recovered Encapsulated Allogenic Islets From Transplanted Diabetic BB/W Rats.* Transplantation, 1992. **54**(4): p. 588-592.

10. Robitaille R., P.J.-F., Leblond F., Lamoureux M., Lepage Y., Halle J-P., *Studies on Small (<350um) Alginate-Poly-L-Lysine Microcapsules. III. Biocompatibility of Smaller vs. Standard Microcapsules.* 1999.

11. de Vos P., d.H.B., van Schilfgaarde R., *Effect of the Alginate Composition on the Biocompatibility of Alginate-Polylysine Microcapsules.* Biomaterials, 1997. **18**: p. 273-278.

12. de Vos P., v.H.C., van Zanten J., Netter S., Strubbe J., Busscher H., *Long-term Biocompatibility, Chemistry, and Function of Microencapsulted Pancreatic Islets.* Biomaterials, 2003. **24**: p. 305-312.

13. Clayton, H., London N., Colloby P., James R., Bell P., *The Effect of Capusle Composition on the Viability and Biocompatibility of Sodium Alginate/Poly-L-Lysine Encapsulated Islets.* Transplantation Proceedings, 1992. **24**(3): p. 956.

14. Schneider S., F.P., Slotty V., Kampfner D., Preuss S., Berger S., Beyer J., Pommersheim R., *Multilayer Capsules: A Promising Microencapsulation System for Transplantation of Pancreatic Islets.* Biomaterials, 2001. **22**: p. 1961-1970.

15. Sadikot R., J.E., Debelak J., Yull F., Christman J., Blackwell TR., Chapman W., Blackwell TS., Zoia O., *High-Dose Dexamethasone Accentuates Nuclear Factor-kB Activation in Endotoxin-Treated Mice.* American Journal of Respiratory and Critial Care Medicine, 2001. **164**: p. 873-878.

16. Blackwell T., C.J., *The Role of Nuclear Factor-kB in Cytokine Gene Regulation.* American Journal of Respiratory Cell and Molecular Biology, 1997. **17**: p. 3-9.

17. Boone, D., Lee E., Shon L., Gibson P., Chien M., Chan F., Madonia M., Burkett P., Ma A., *Recent Advances in Understanding NF-kB Regulation.* Inflammatory Bowel Diseases, 2002. **8**(3): p. 201-212.

18. Christman J., S.R., Blackwell T., *The Role of Nuclear Factor-kB in Pulmonary Diseases.* Chest, 2000. **117**(5): p. 1482-1487.

19. Sadikot R., H.w., Everhart M., Zoia O., Peebles R., Jansen E., Yull F., Christman J., Blackwell T., *Selective IkB Kinase Expression in Airway Epithelium Generates Neutrophilic Lung Inflammation.* The Journal of Immunology, 2003. **170**: p. 1091-1098.

20. Gray K., S.M., Chapman W., Blackwell T., Christman J., Washington M., Yull F., Jaffal N., Jansen D., Gautman S., Stain S, *Systemic NF-kB Activation in a Transgenic Mouse Model of Acute Panreatitis.* Journal of Surgical Research, 2003. **110**: p. 310-314.

21. Klement J., R.N., Car B., Abbondanzo S., Powers G., Bhatt H., Chen C-H., Rosen C., Stewart C., *IkBalpha Deficiency Results in a Sustained NF-kB Response and Severe Widespread Dermatitis in Mice.* Molecular and Cellular Biology, 1996. **16**(No. 5): p. 2341-2349.

22. Black, J., *Biological Performance of Materials: Fundamentals of Biocompatibility*. Third Edition, Revised and Expanded ed. 1999, New York: Marcel Dekker, Inc.

23. Dirsch V., K.H., Vollmar A., *Garlic Metabolites Fail to Inhibit the Activation of the Transcription Factor NF-kB and Subsequent Expression of the Adhesion Molecule E-Selectin in Human Endothelial Cells.* European Journal of Nutrition, 2004. **43**: p. 55-59.

24. Collins T., C.M., *NF-kB: Pivotal Mediator or Innocent Bystander in Atherogenesis?* The Journal of Clinical Investigation, 2001. **107**(3): p. 255-264.

25. Gille J., P.L., Lawley T., Caughman S., Swerlick R., *Retinoic Acid Inhibits the Regulated Expression of Vascular Cell Adhesion Molecule-1 by Cultured Dermal Microvascular Endothelial Cells.* Journal of Clinical Investigation, 1997. **99**(3): p. 492-500.

26. Lopez-Cabrera M., N.A., Vara A., Garcia-Aguilar J., Tugores A., Corbi A., *Characterization of the p150,95 Leukocyte Integrin alpha Subunit (CD11c) Gene Promoter.* The Journal of Biological Chemistry, 1993. **268**(2): p. 1187-1193.

27. Epstein, R., *Human Molecular Biology: An Introduction to the Molecular Basis of Health and Disease*. First Edition ed. 2003, Cambridge: Press Syndicate of the University of Cambridge.

28. Campbell, N., *Biology*. Fourth Edition ed. 1996, Menlo Park, California: The Benjamin/Cummings Publishing Company, Inc.

29. Koay M., G.X., Washington M., Parman K., Sadikot T., Blackwell T., Christman J., *Macrophages are Necessary for Maximal Nuclear Factor-kB Activation in Response to Endotoxin.* American Journal of Respiratory Cell and Molecular Biology, 2002. **26**(Number 5): p. 572-578.

30. Gill, R., *Antigen Presentation Pathways for Immunity to Islet Trnasplants: Relevance to Immunoisolation.* Annals New York Academy of Sciences, 1999. **875**: p. 255-260.

31. Gray, D., *An Overview of the Immune System with Specific Referance to Membrane Encapsulation and Islet Transplantation.* Annals New York Academy of Sciences, 2001. **944**: p. 226-239.

32. Weber C., Z.S., Koschitzky T., Wicker L., Rajotte R., D'Agati V., Peterson L. Norton J., Reemtsma K., *The Role of CD4+ Helper T Cells in the Destruction of Microencapsulated Islet Xenografts in NOD Mice.* Transplantation, 1990. **49**(2): p. 396-404.

33. Horney B., M.A., Zlotnik A., *Chemokines: Agents for the Immunotherapy of Cancer?* Nature, 2002. **2**(March): p. 175-183.

34. Richmond, A., *NF-kB, Chemokine Gene Transcription and Tumor Growth.* Nature, 2002. **2**(September): p. 664-672.

35. Brantley D., C.C.-L., Muraoka R., Bushdid P., Bradberry J., Kittrell F., Medina D., Matrisian L., Kerr L., Yull F., *Nuclear Factor-kB Regulates Proliferation and Branching in Mouse Mammary Epithelium.* Molecular Biology of the Cell, 2001. **12**: p. 1445-1455.

36. Chen C-L., S.N., Yull F., Strayhorn D., Kaer L., Kerr L., *Lymphocytes Lacking IkB-alpha Develop Normally, But Have Selective Defects in Proliferation and Function.* The Journal of Immunology, 2000. **165**: p. 5418-5427.

37. Chen C-L., Y.F., Cardwell N., Singh N., Strayhorn W., Nanney L., Kerr L., *RAG2 -/-, IkB-alpha -/- Chimeras Display a Psoriasiform Skin Disease.* The Journal of Investigative Dermatology, 2000. **115**: p. 1124-1133.

38. Hu Y., B.V., Delhase M., Zhang P., Deerinck T., Ellisman M., Johnson R., Karin M., *Abnormal Morphogenesis But Intact IKK Activation in Mice Lacking the IKKalpha Subunit of IkB Kinase.* Science, 1999. **284**: p. 316-320.

39. Schneider C., S.D., Brantley D., Nanney L., Yull F., Brash A., *Upregulation of 8-Lipoxygenase in the Dermatitis of IkB-alpha-Deficient Mice.* The Journal of Investigative Dermatology, 2004. **122**: p. 691-698.

40. Takeda K., T.O., Tsujimura T., Itami S., Adachi O., Kawai T., Sanjo H., Yoshikawa K., Terada N., Akira S., *Limb and Skin Abnormalities in Mice Lacking IKKalpha.* Science, 1999. **284**: p. 313-316.

41. Li Q., L.Q., Hwang J., Buscher D., Lee K-F., Izpisua-Belmonte J., Verma I., *IKK1-deficient Mice Exhibit Abnormal Development of Skin and Skeleton.* Genes and Development, 1999. **13**: p. 1322-1328.

42. Kunsch C., R.S., Rosen C., *Selection of Optimal kB/Rel DNA-Binding Motifs; Interaction of Both Subunits of NF-kB with DNA is Required for Transcriptional Activation.* Molecular and Cellular Biology, 1992. **12**: p. 4412-4421.

43. Hastings, J.W., *Chemistries and Colors of Bioluminescent Reactions: A Review.* Gene, 1996. **173**: p. 5-11.

44. Ugarova N., B.L., *Protein Structure and Bioluminscent Spectra for Firefly Biolumiscence.* Luminescence, 2002. **17**: p. 321-330.

45. Sadikot R., W.L., Jansen E., Debelak J., Yull F., Christman J., Blackwell T., Chapman W., *Hepatic Cryoablation-Induced Multisystem Injury: Bioluminescent Detection of NF-kB Activation in a Transgenic Mouse Model.* Journal of Gastrointestinal Surgery, 2002. **6**(2): p. 264-270.

46. Oba O., O.M., Inouye S., *Firefly Luciferase is a Bifuntional Enzyme: ATP-dependent Monooxygenase and a Long Chain Fatty Acyl-CoA Synthetase.* Federation of European Biochemical Societies Letters, 2003. **540**: p. 251-254.

47. Blackwell TS., Y.F., Chen C., Venkatakrishman A., Blackwell TR., Hicks D., Lancaster L., Christman J., Kerr L., *NF-kB Activation and Cytokine Production in a Transgenic Mouse Model of Endotoxin-Induced Lung Inflammation.* American Journal of Respiratory and Critial Care Medicine, 2000. **162**: p. 1095-1101.

48. de Vos P., v.S.R., *Factors Influencing the Properties and Performance of Microcapsules for Immunoprotection of Pancreatic Islets.* Journal of Molecular Medicine, 1999. **77**: p. 199-205.

49. Anilkumar A., L.I., Wang T., *A Novel Reactor for Making Uniform Capsules.* Biotechnology and Bioengineering, 2001. **75**(5): p. 581-589.

50. Pariseau J-F., L.F., Harel F., Lepage Y., Halle J-P., *The Rat Epididyman Fat Pad as an Implantation Site for the Study of Microcapsule Biocompatibility: Validation of the Method.* Journal of Biomedical Materials Research, 1995. **29**: p. 1331-1335.

51. Lacik I., B.M., Anilkumar A., Powers A., Wang T., *New Capsule with Tailored Properties for the Encapsulation of Living Cells.* Journal of Biomedical Materials Research, 1998. **39**: p. 52-60.

52. De Vos P., D.H.B., van Schilfgaarde R., Wolters G., *Factors Influencing the Adequacy of Microencapsulation of Rat Pancreatic Islets.* Transplantation, 1996. **62**(7): p. 888-893.

53. Rosinski S., G.G., Lewinska D., Ritzen L., Vierstein H., Teunou E., Poncelet D., Zhang Z., Fan X., Serp D., Marison I., Hunkeler D., *Characterization of Microcapsules: Recommended Methods Based on Round-Robin Testing.* Journal of Microencapsulation, 2002. **19**(5): p. 641-659.

54. Strand B., G.O., Kulseng B., Espevik T., Skjak-Braek G., *Alginate-polylysine-alginate Microcapsules: Effect of Size Reduction on Capsule Properties.* Journal of Microencapsulation, 2002. **19**(5): p. 615-630.